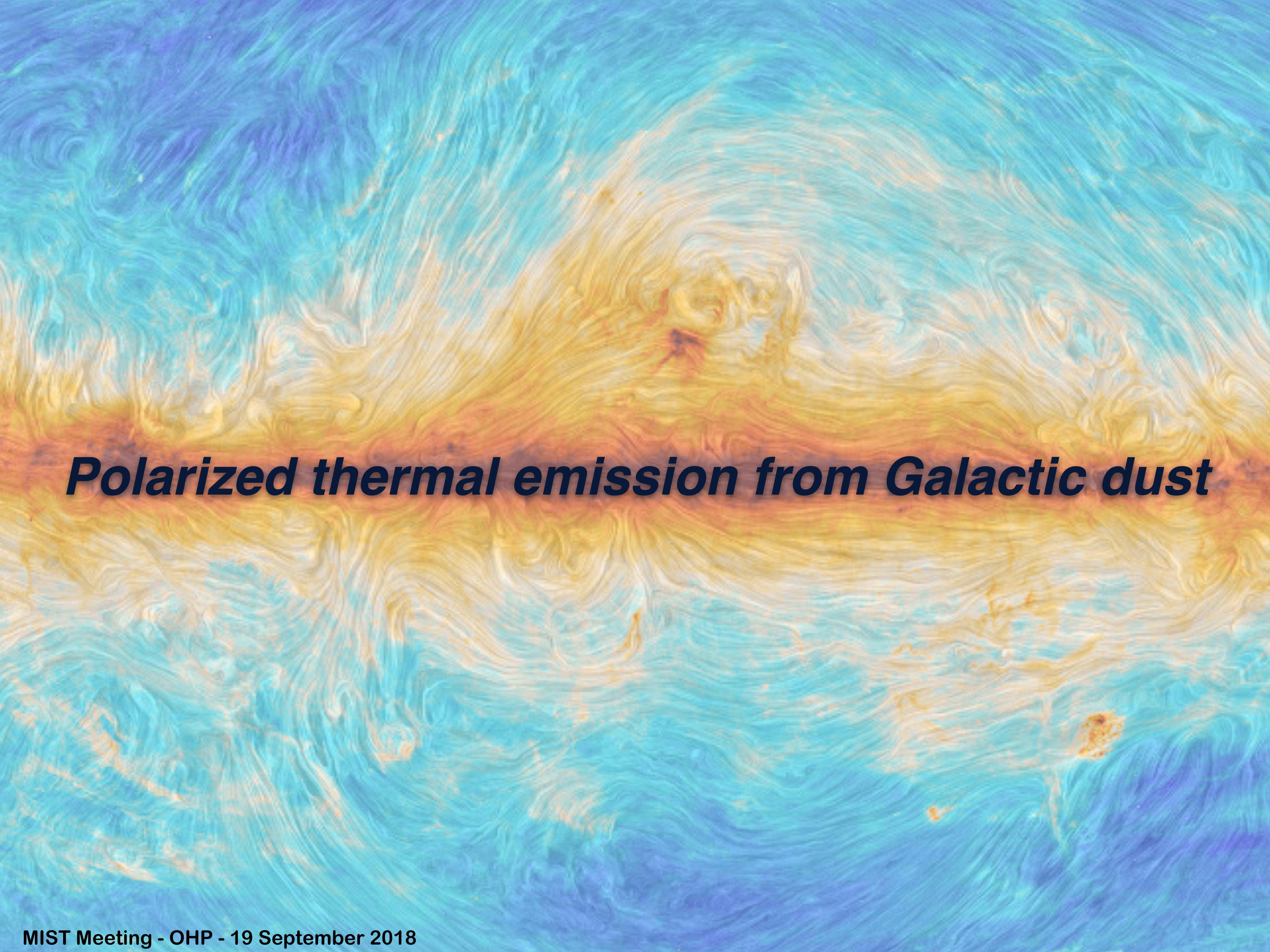

Polarized thermal emission from Galactic dust

The Planck mission

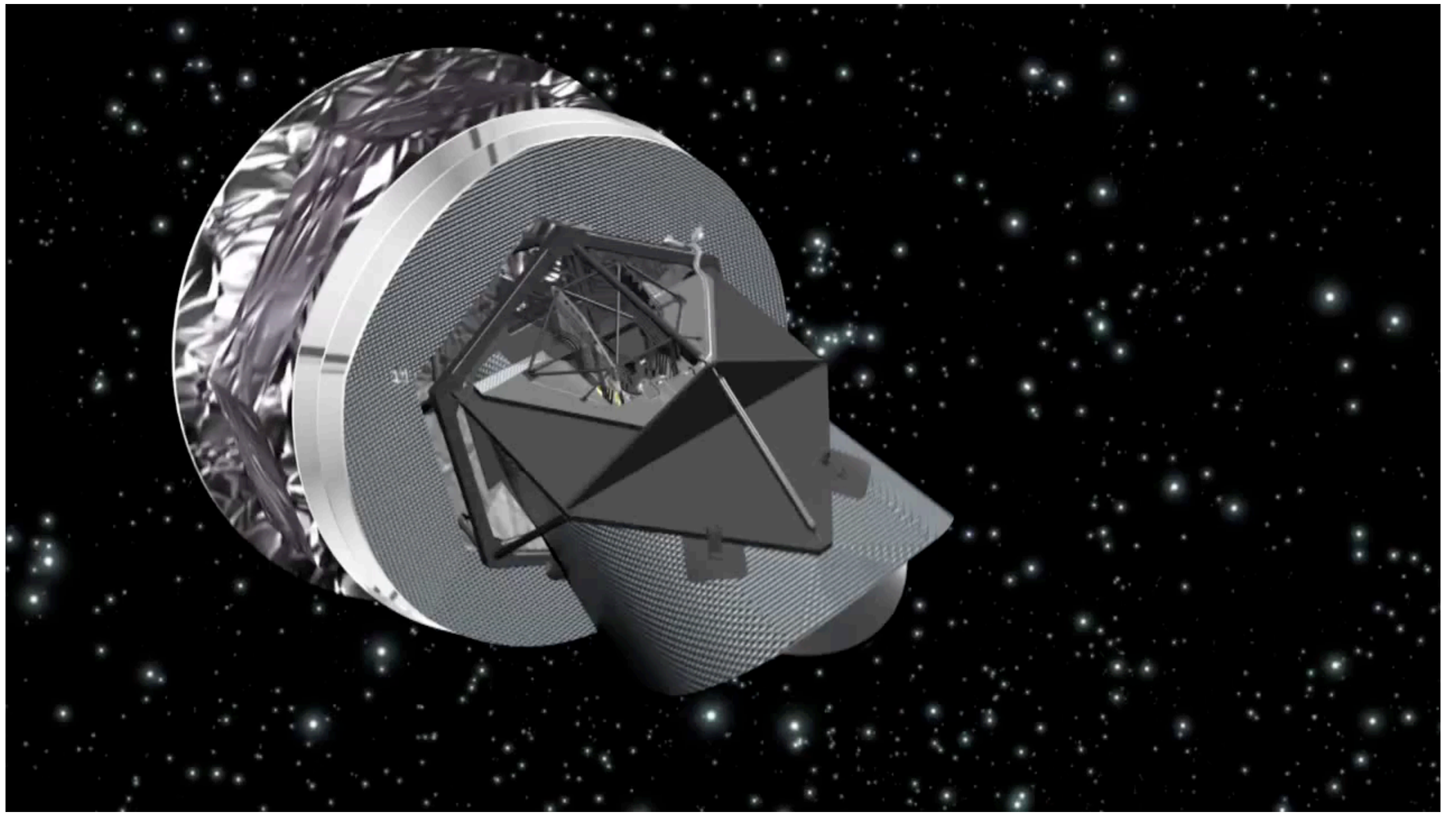

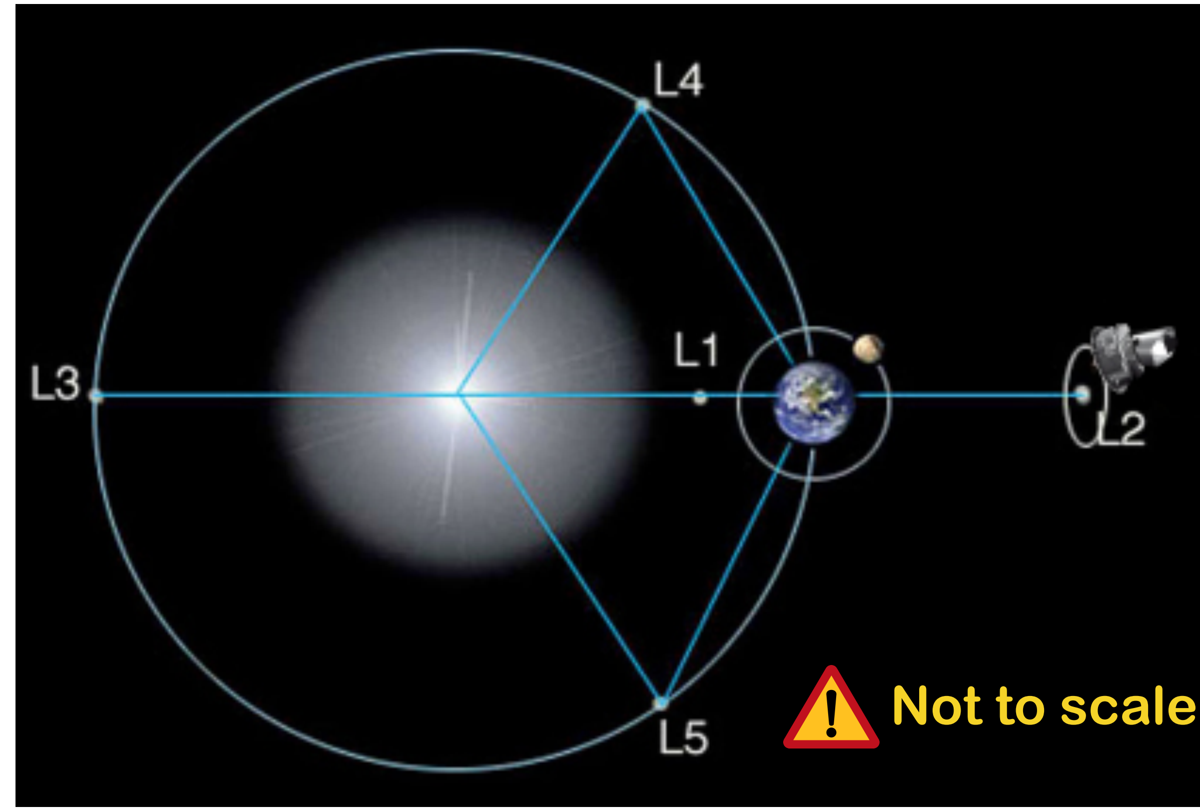

- 2009-2013 European space mission : Full survey of the microwave sky
- 30 - 857 GHz coverage in nine bands
- Measurement of Cosmic Microwave Background (CMB) anisotropies
- Mapping of the cold, dusty Milky Way
- First full-sky survey in microwave polarization

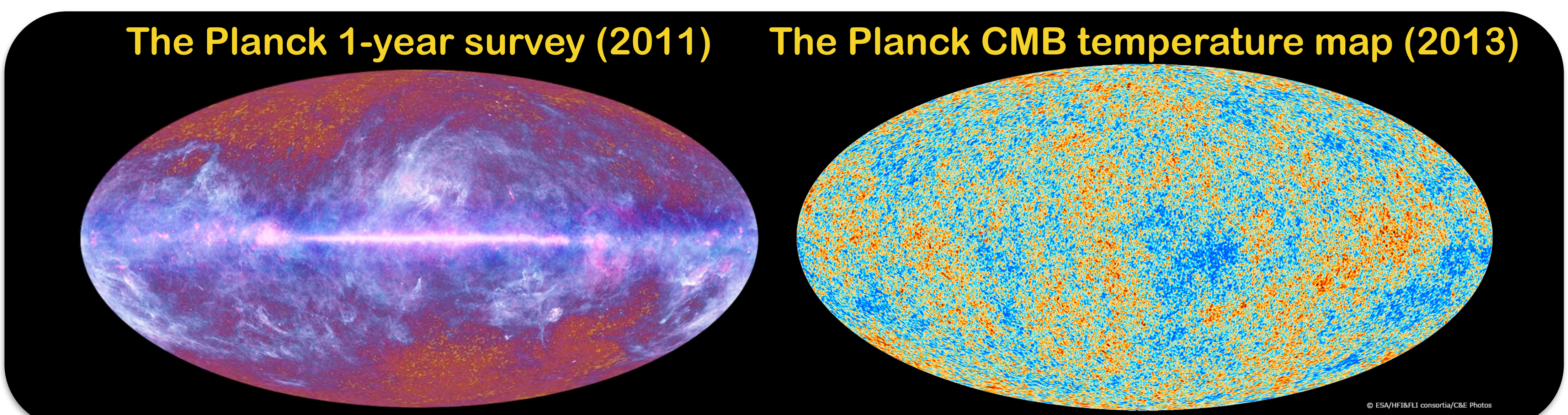

Galactic dust emission : a foreground to the CMB

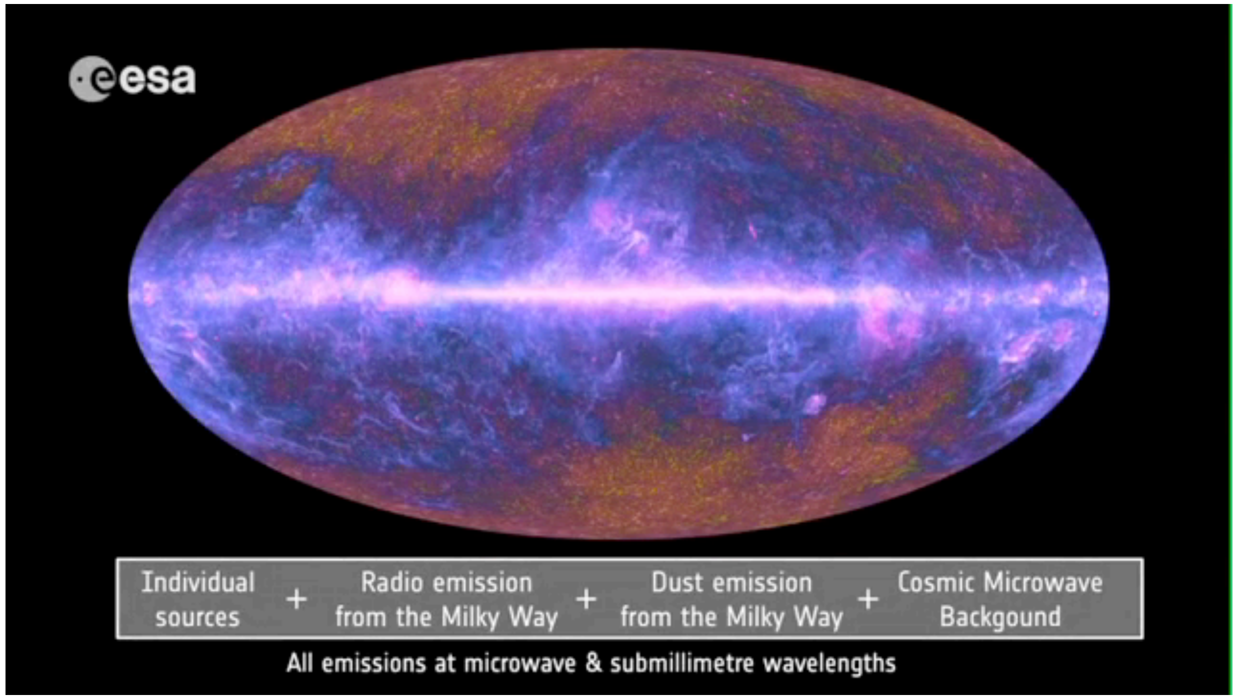

Total intensity

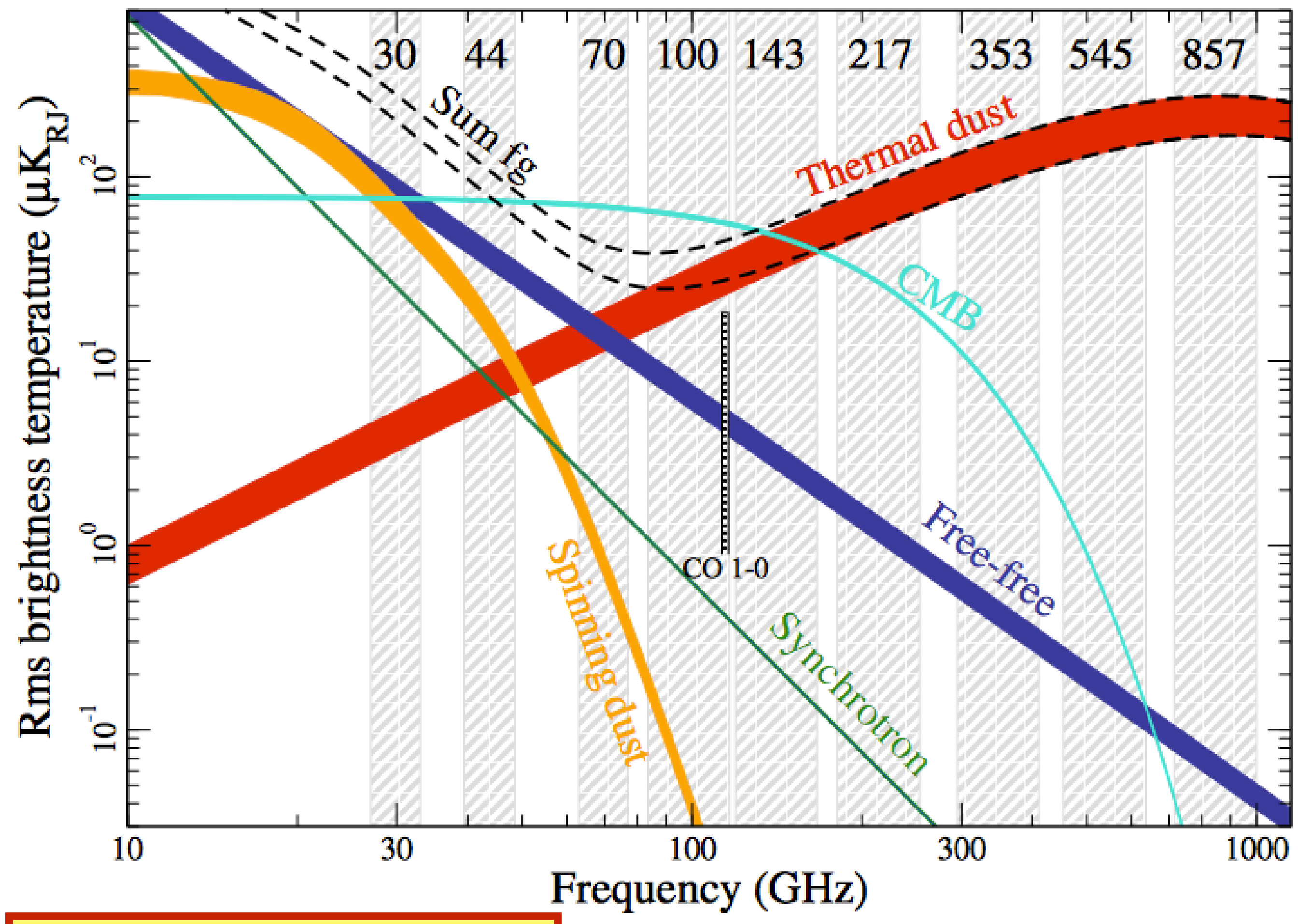

Polarized intensity

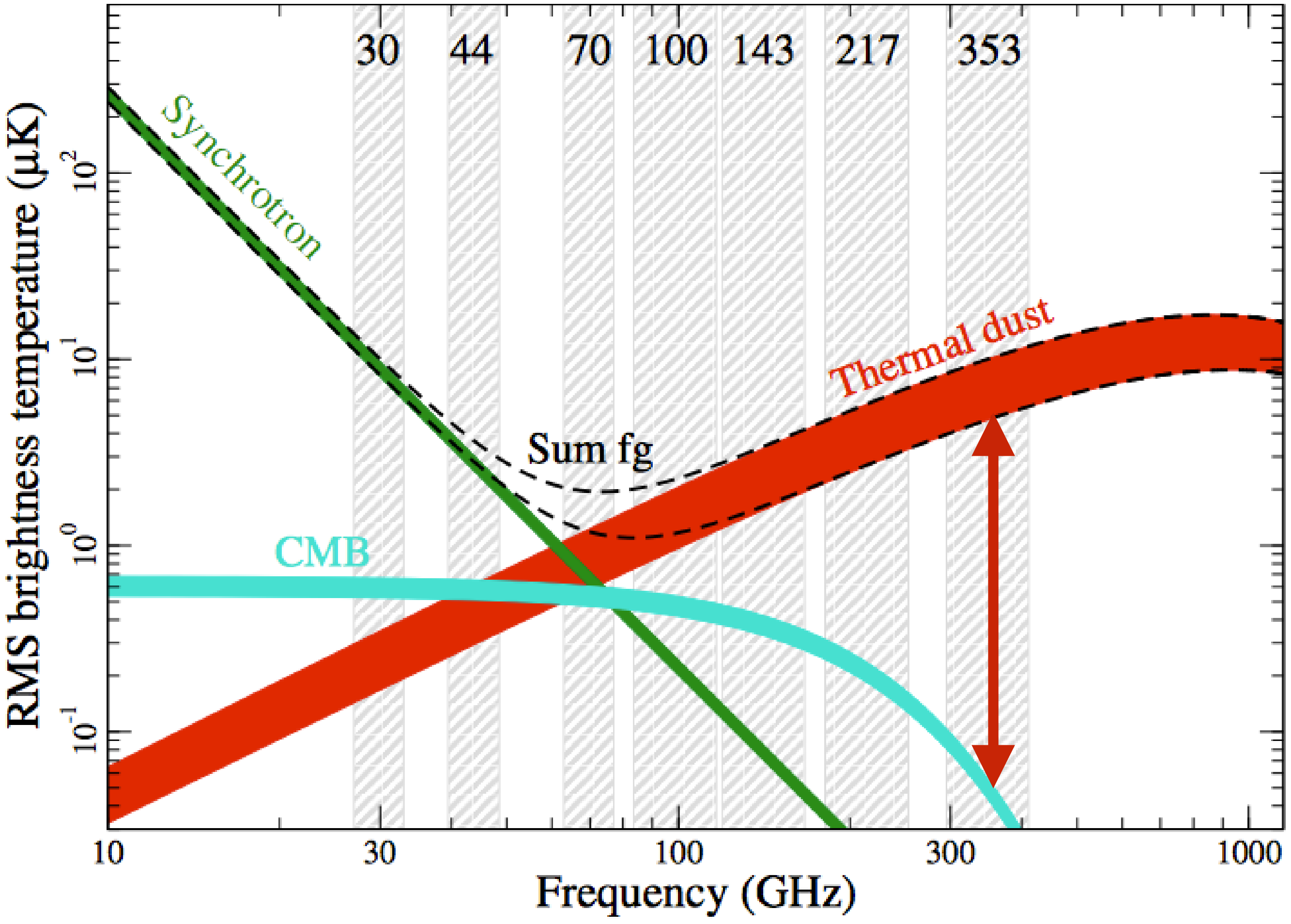

Planck Collaboration I (2016)

Interstellar dust emission

UV and visible absorption

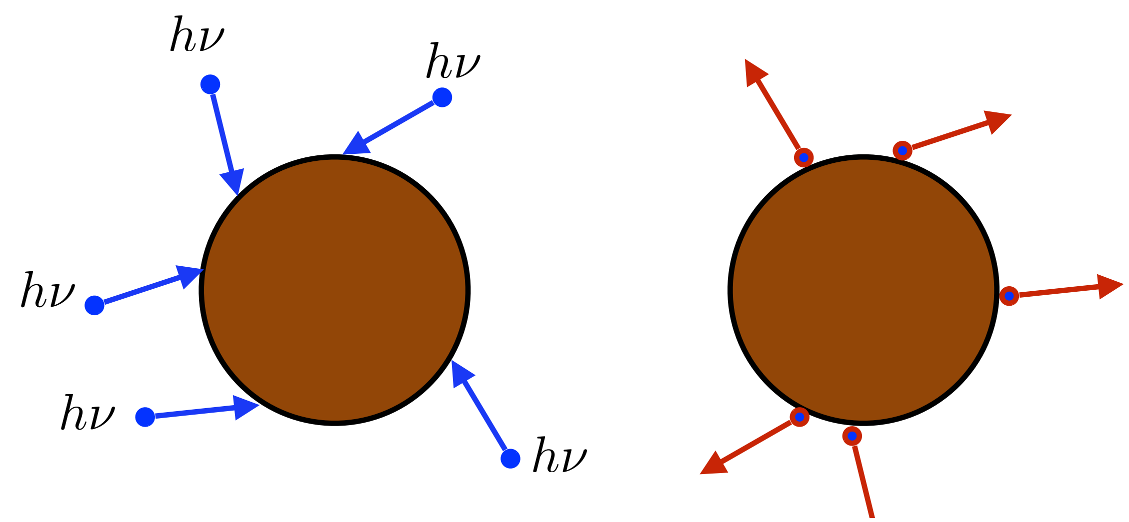

Infrared emission (~ 10 K)

Large grains at equilibrium

$$\int \kappa_\nu J_\nu \mathrm{d}\nu = \int \kappa_\nu B_\nu (T_\mathrm{d})\, \mathrm{d}\nu$$

← *Grain temperature*

Example

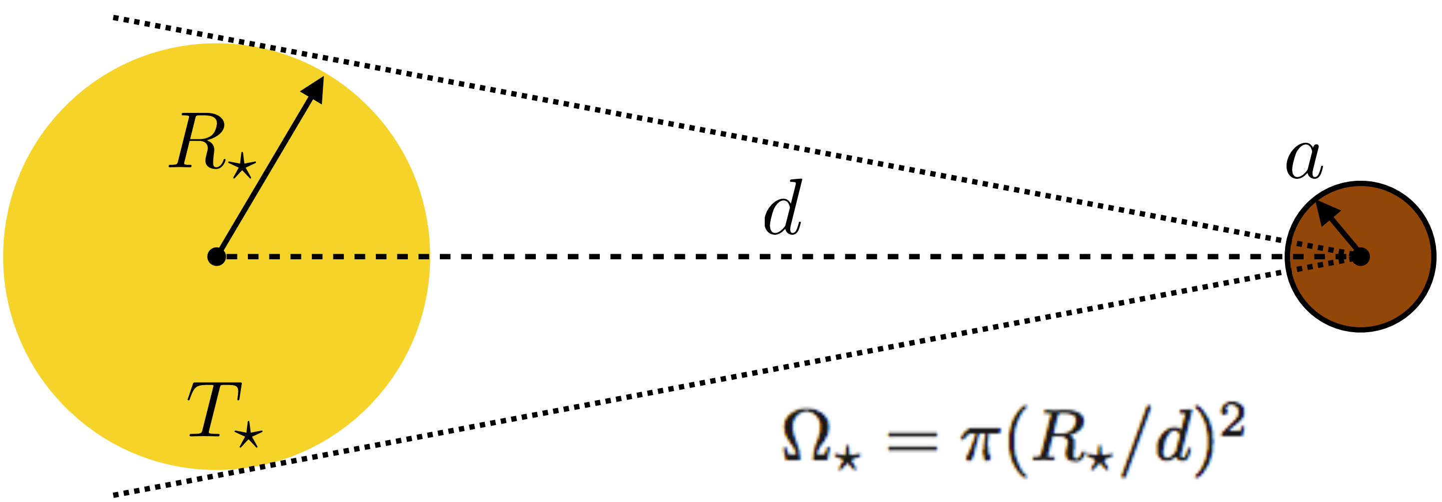

$$\Omega_\star = \pi (R_\star / d)^2$$

Equilibrium temperature

$$T_\mathrm{d} = C_\beta \left[\frac{T_\star^4}{a} \left(\frac{R_\star}{d} \right)^2 \right]^{1/(4+\beta)}$$

Spectral index in the IR $\beta \simeq 1 - 2$

$$\delta T \sim \frac{h\nu}{C}$$

Interstellar dust emission

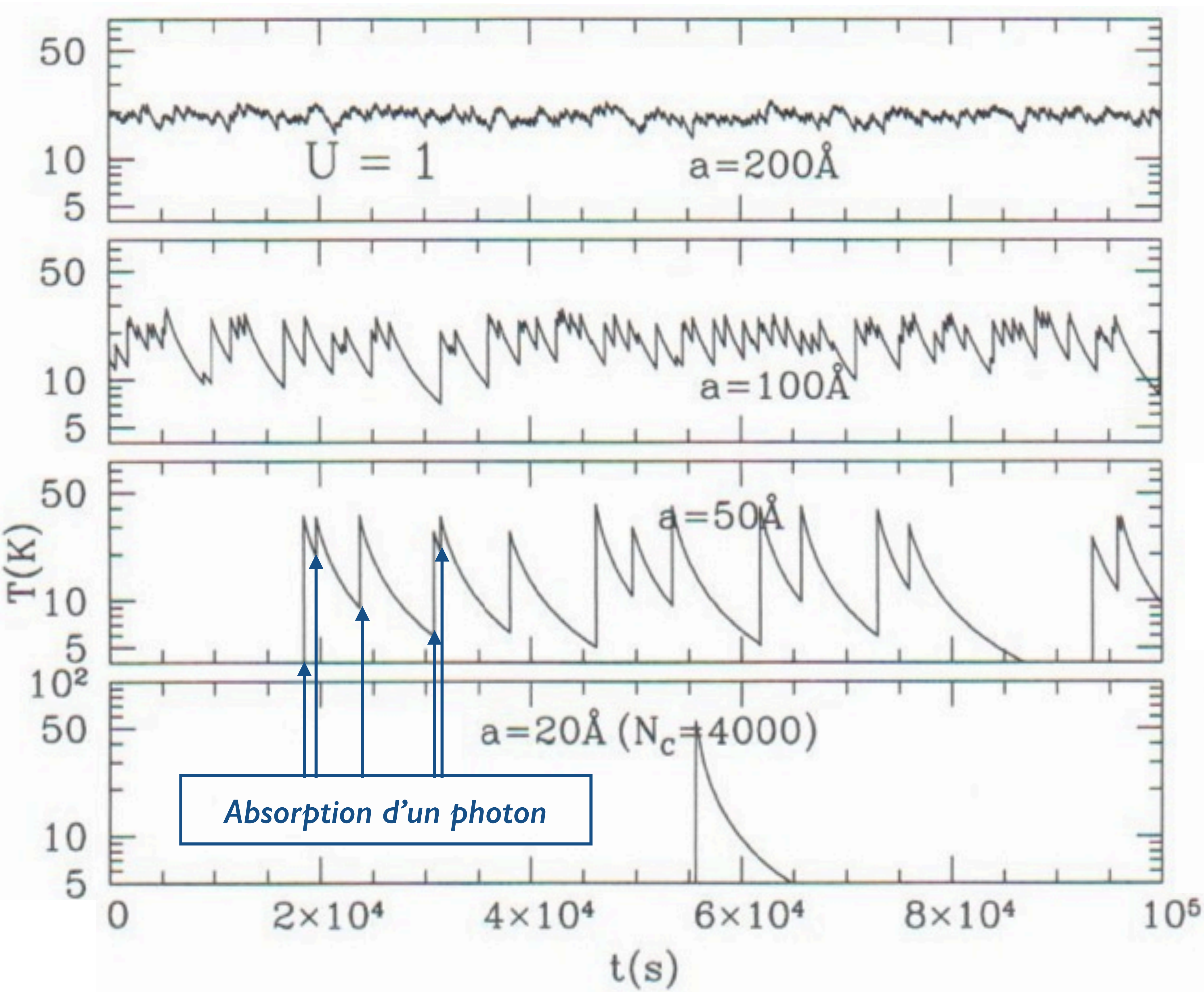

Draine, 2011, « Physics of the Interstellar and Intergalactic Medium »

Magnetic fields in the Milky Way

Beck (2016)

- Coupled to the gas, provides balance with gravity, controls the propagation of cosmic rays
- Generated from primordial seed fields via a coupling of differential rotation and Coriolis force
- Superposition of a large-scale field following spiral arms and of a turbulent component

Field reversals

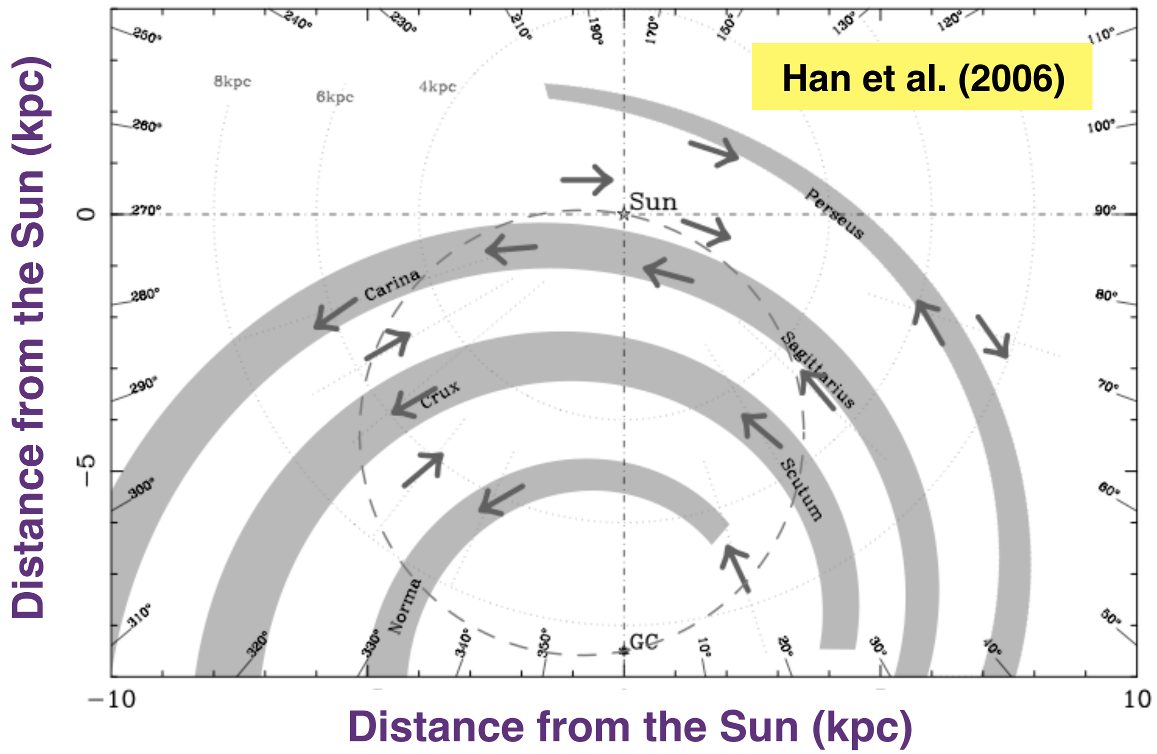

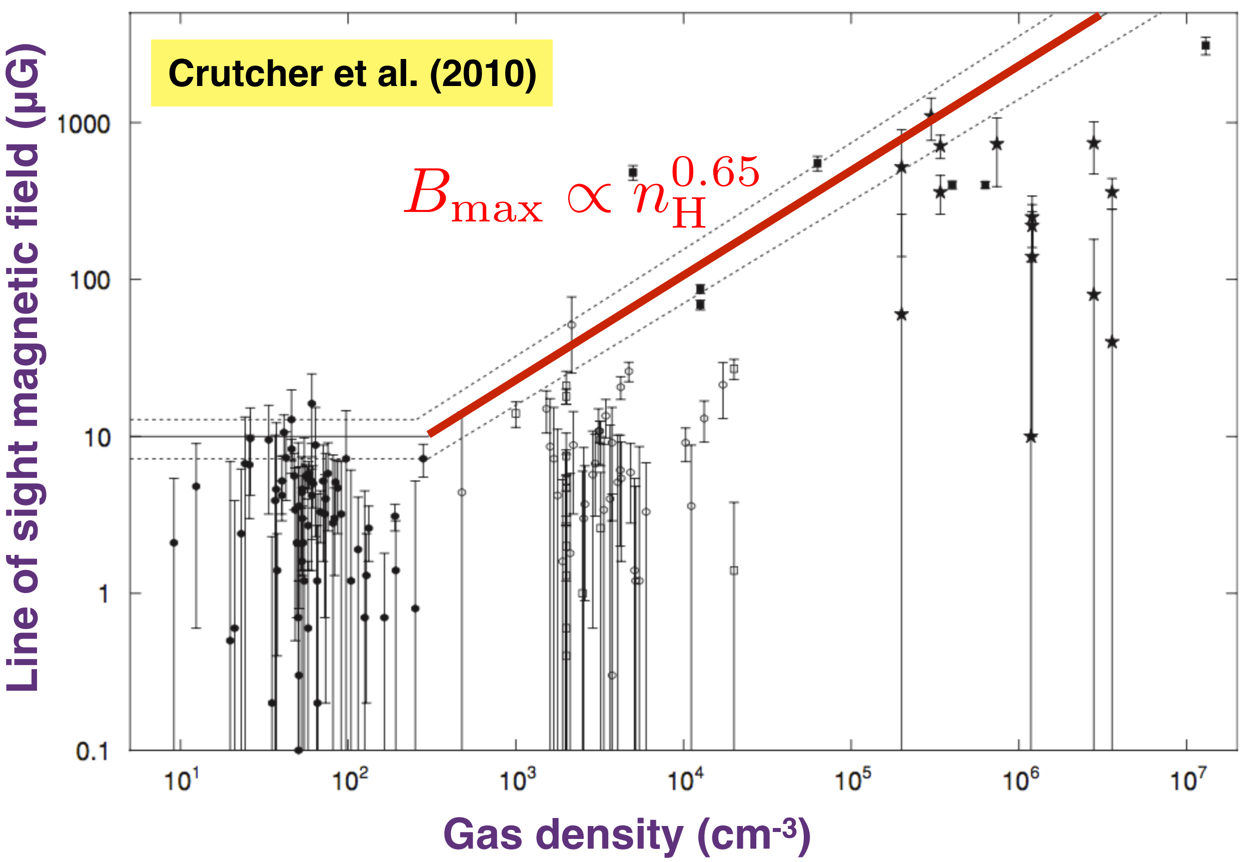

$$B = B_0 + B_t$$

$B_0 \sim$ a few μG; $B_t \sim$ a few μG

Haverkorn et al. (2008)

Measurement methods

Notation	Observational signatures
$B^2_{\rm tot,\perp} = B^2_{\rm turb,\perp} + B^2_{\rm reg,\perp}$	Total synchrotron intensity
$B^2_{\rm turb,\perp} = B^2_{\rm iso,\perp} + B^2_{\rm aniso,\perp}$	Total synchrotron emission, partly polarized
$B_{\rm iso,\perp}\ (= \sqrt{2/3}\,B_{\rm iso})$	Unpolarized synchr. intensity, beam depolarization, Faraday depolarization
$B_{\rm iso,\parallel}\ (= \sqrt{1/3}\,B_{\rm iso})$	Faraday depolarization
$B^2_{\rm ord,\perp} = B^2_{\rm aniso,\perp} + B^2_{\rm reg,\perp}$	Intensity and vectors of radio, optical, IR & submm pol.
$B_{\rm aniso,\perp}$	Intensity and vectors of radio, optical, IR & submm pol., Faraday depolarization
$B_{\rm reg,\perp}$	Intensity and vectors of radio, optical, IR & submm pol., Goldreich-Kylafis effect
$B_{\rm reg,\parallel}$	Faraday rotation + depol., longitudinal Zeeman effect

Dust, magnetic fields and polarization

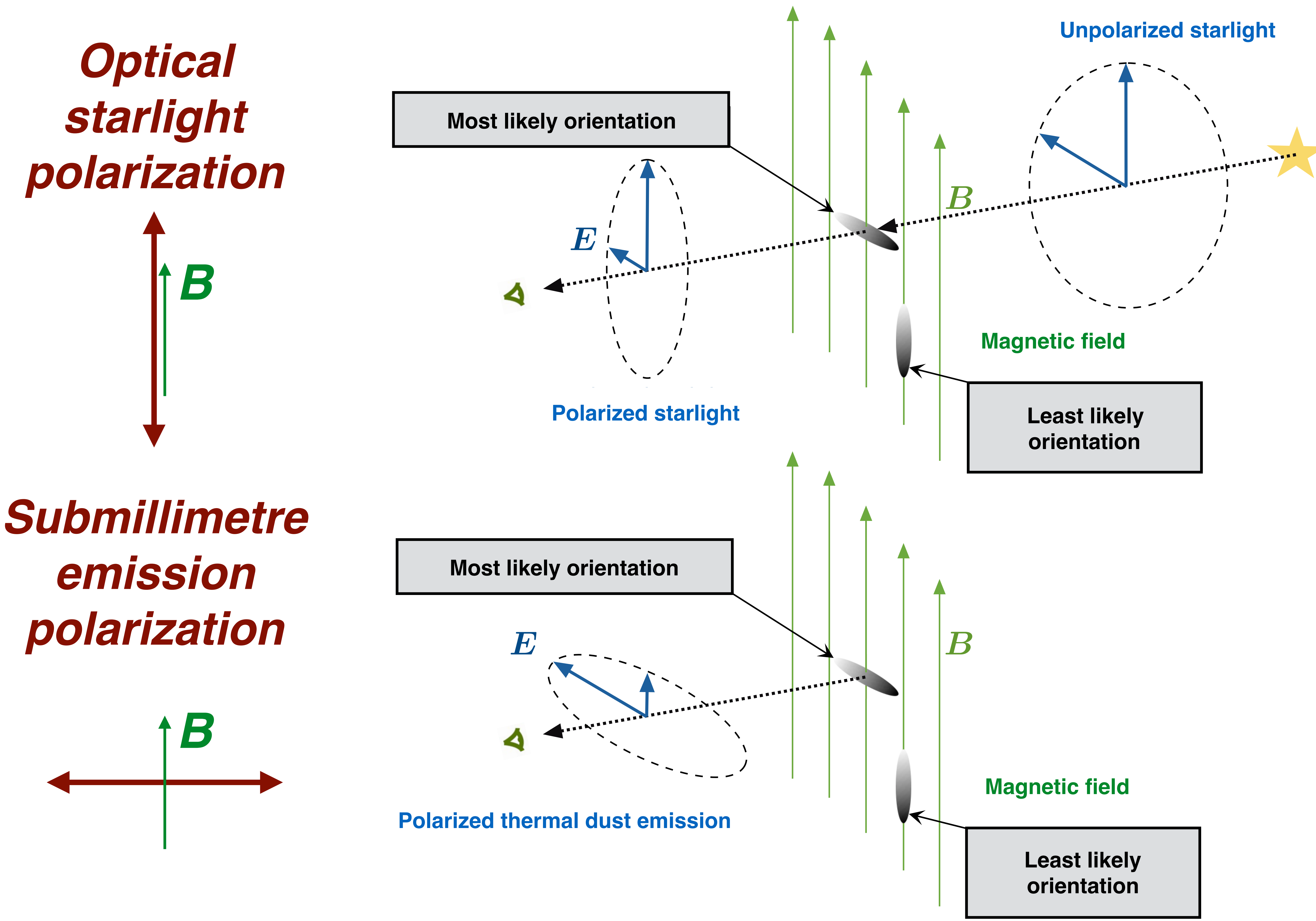

Starlight polarisation

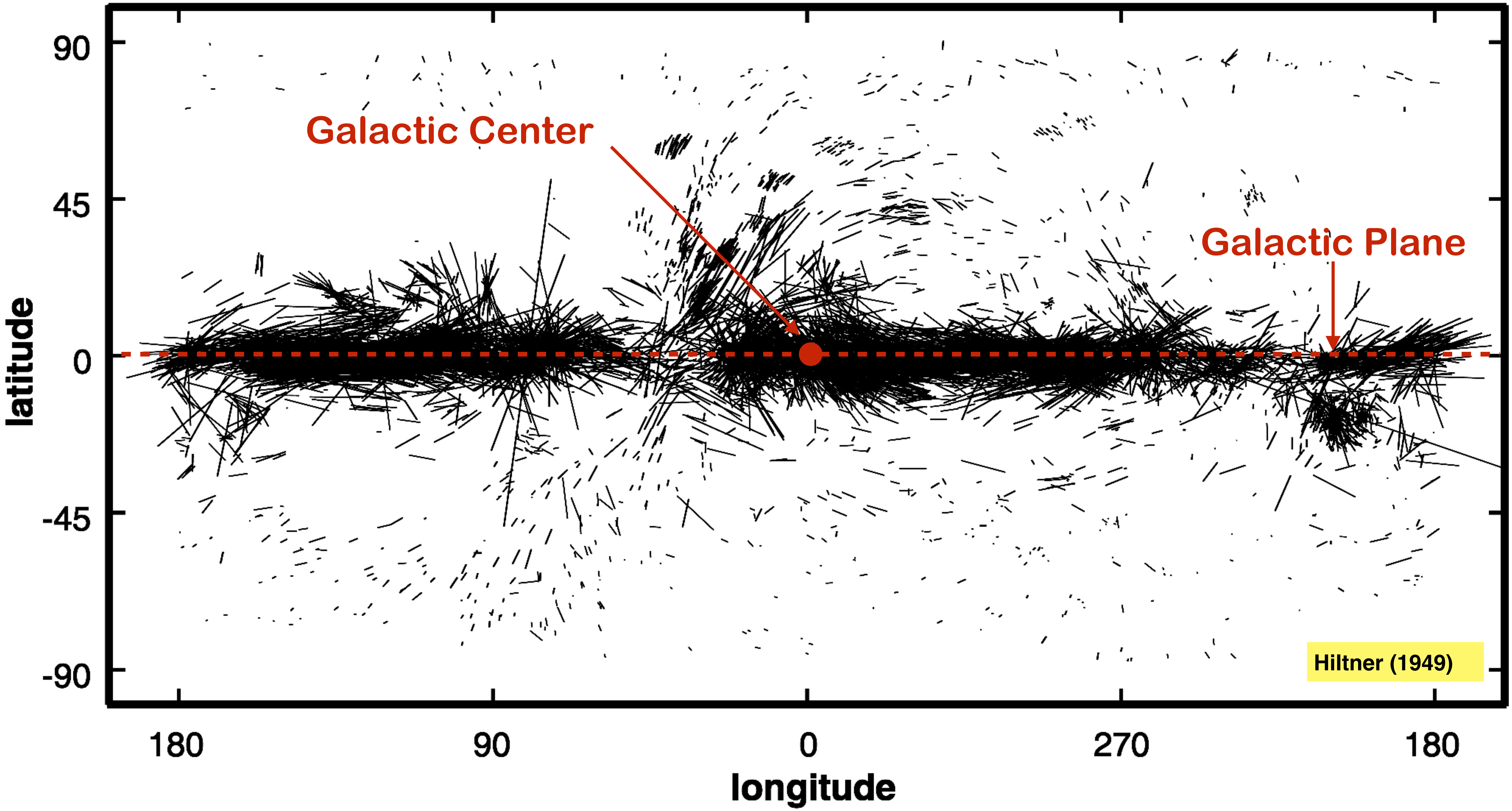

Starlight polarization direction = Plane-of-the-sky orientation of B

Stokes parameters, E and B modes

Stokes Parameters

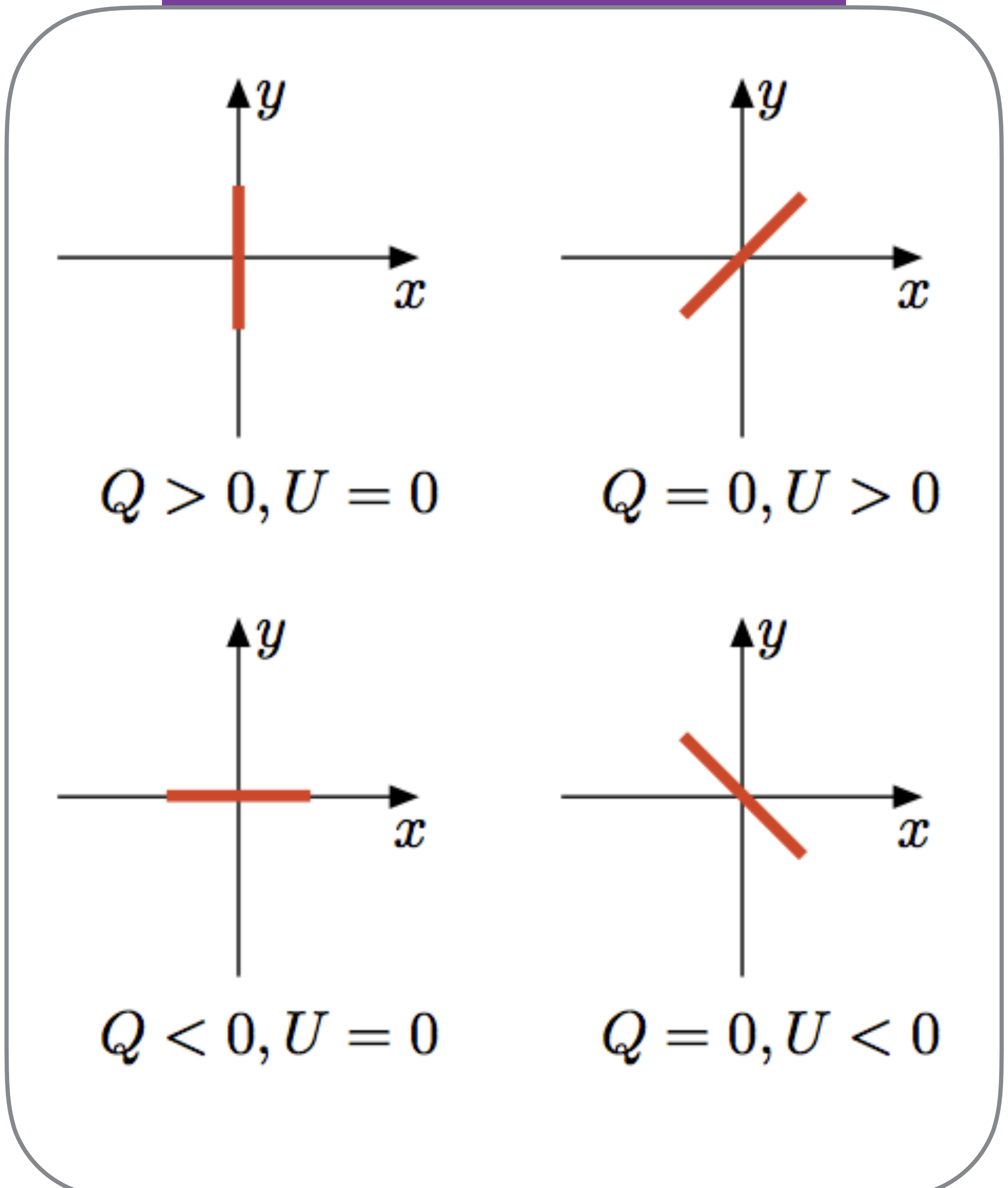

E- and B-modes

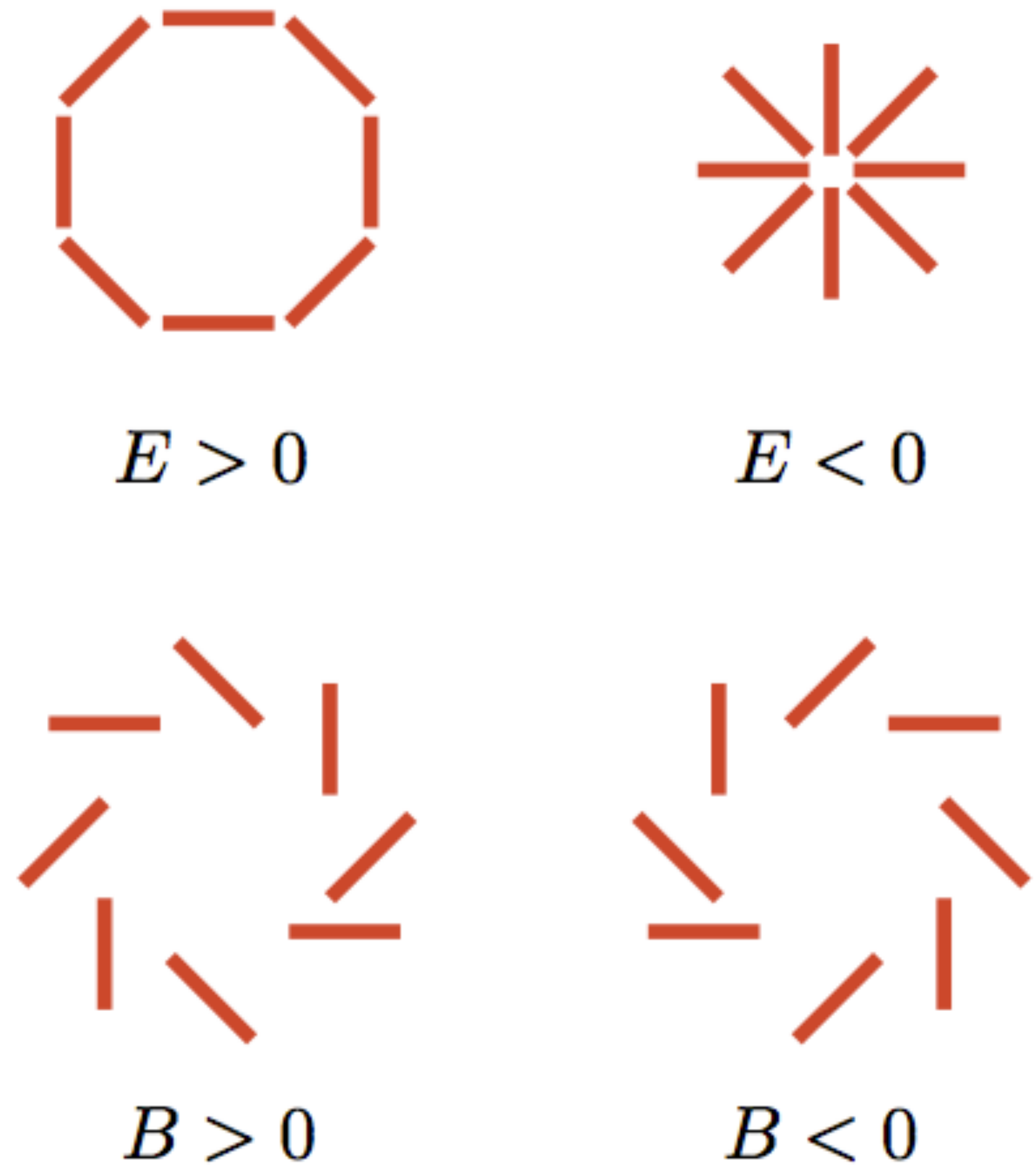

Polarized thermal dust emission at 353 GHz

- GNILC processing reduces noise, CMB, CIB contamination
- Maps available at varying resolution (5’ to 80’)
- Analysis performed on uniform 80’ resolution maps

Planck Collaboration XII (in prep)
Remazeilles et al. (2011)
Planck Collaboration Int XLVIII (2016)

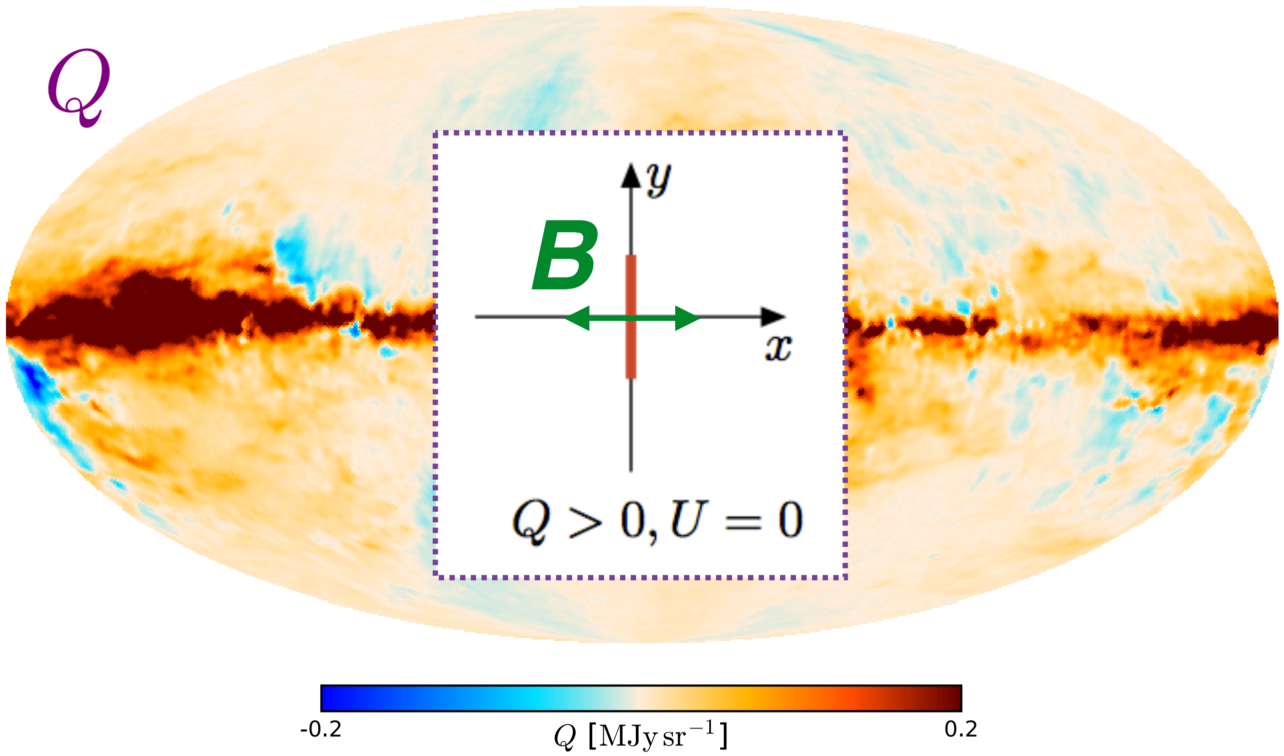

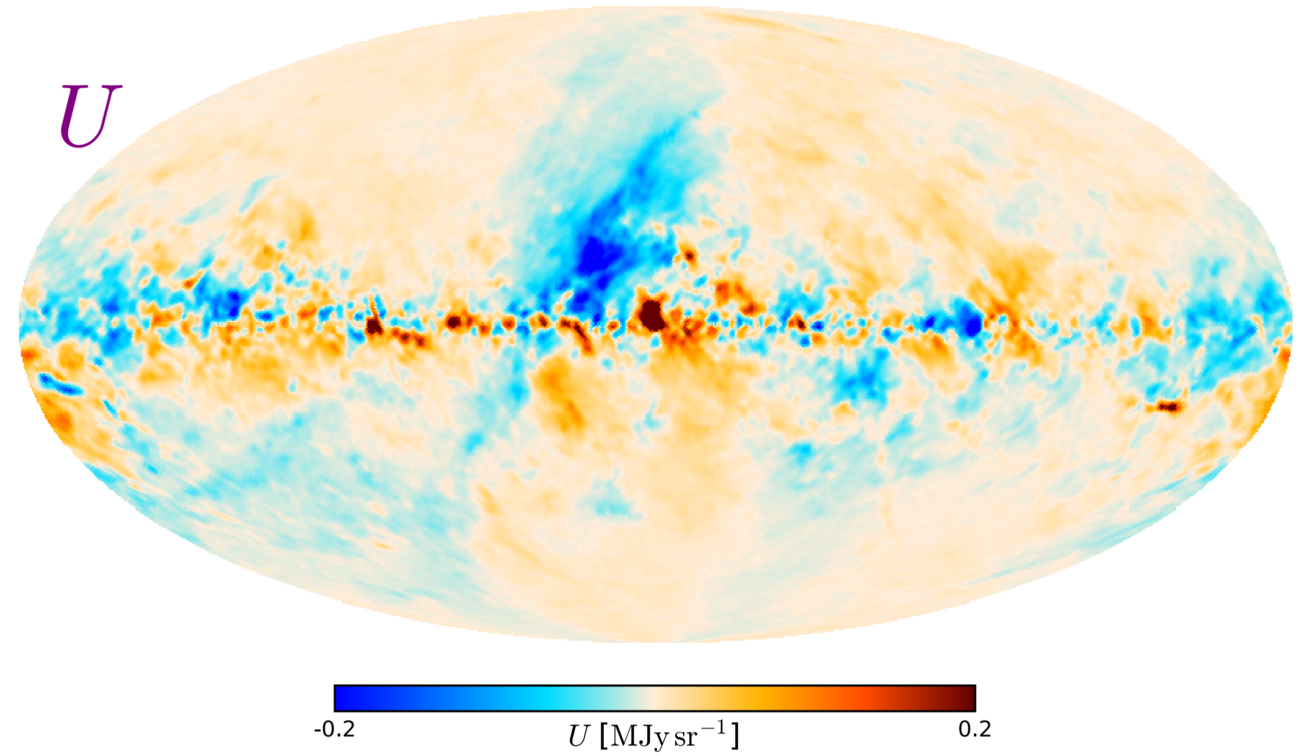

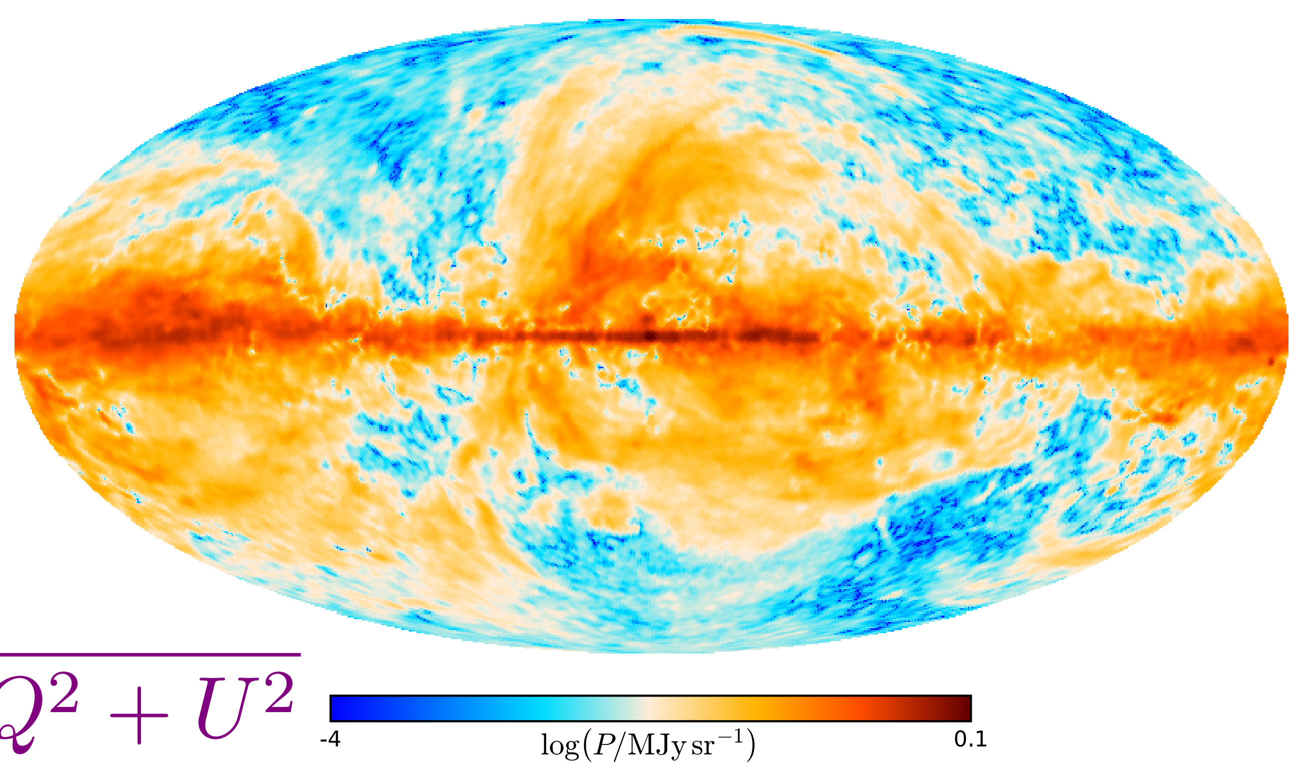

$$P = \sqrt{Q^2 + U^2}$$

Polarized and total intensities

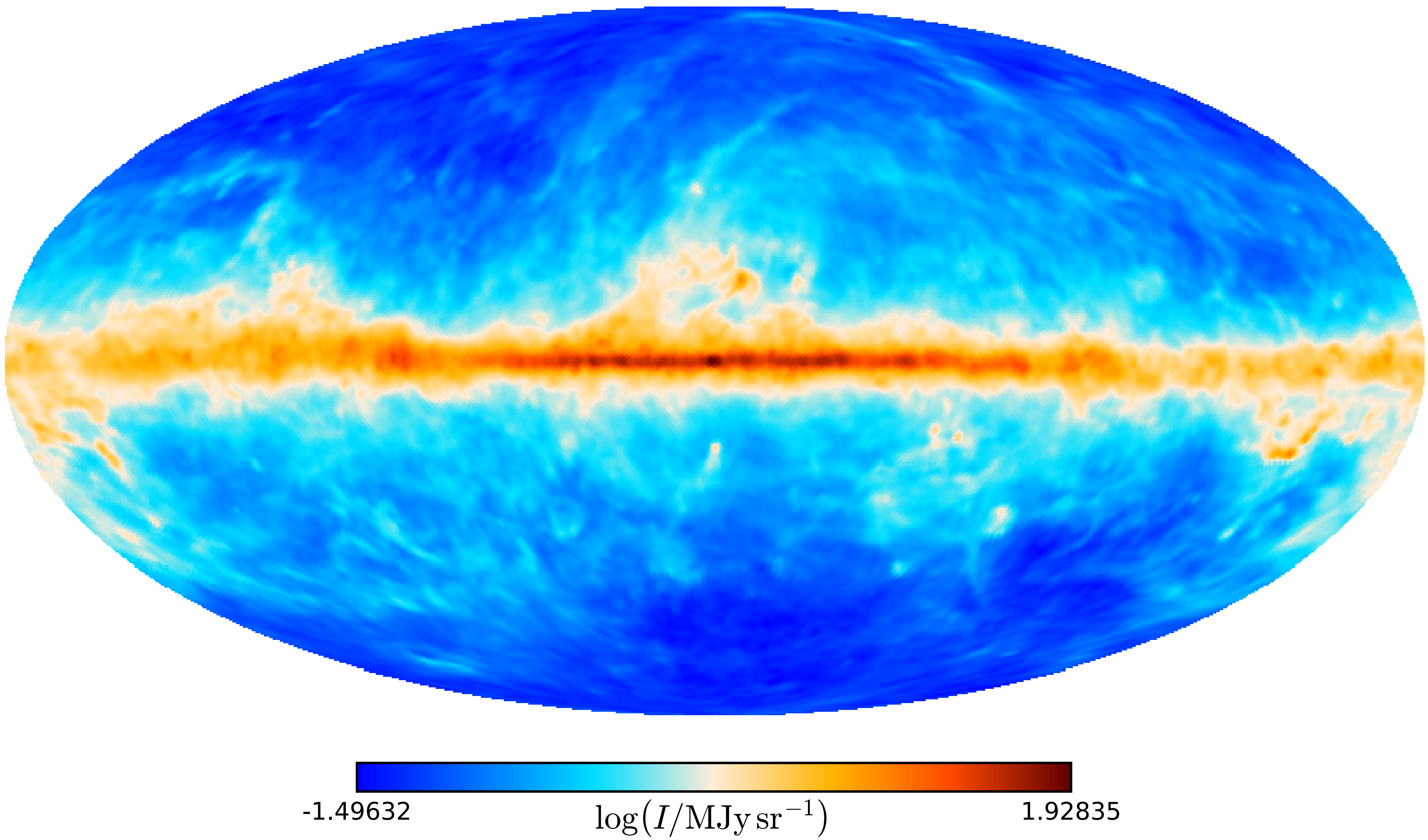

Polarization fraction and angle

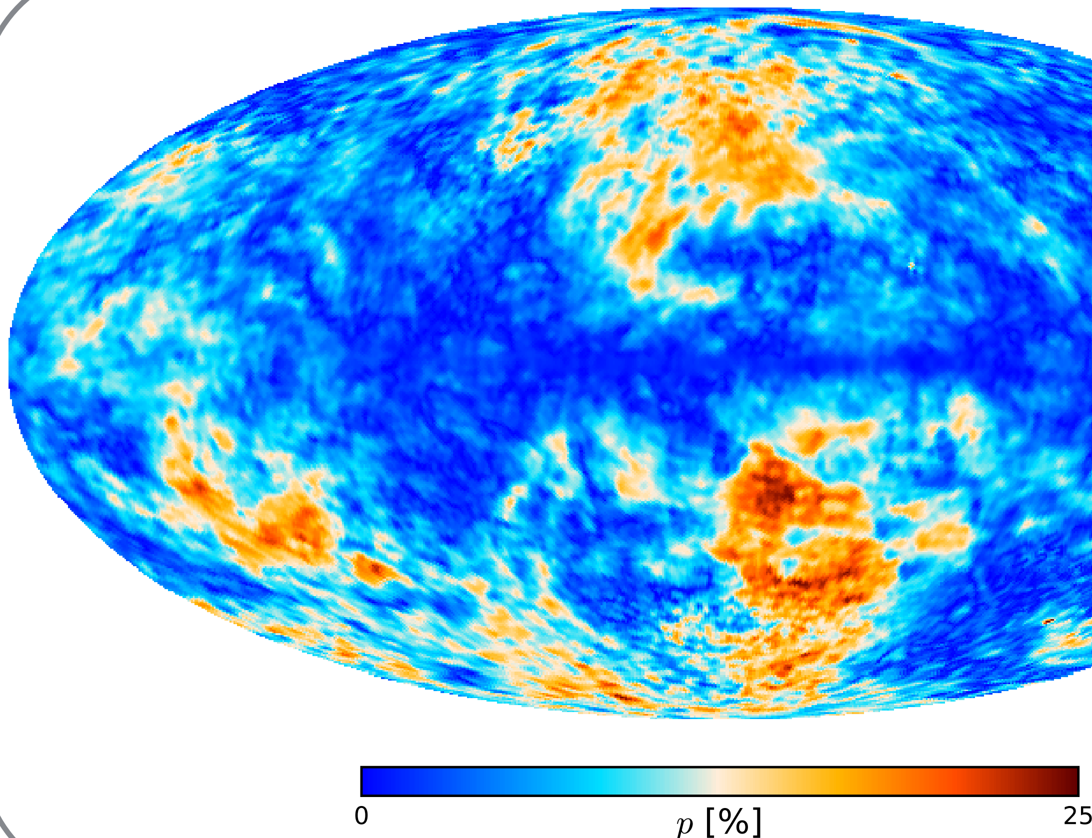

Polarization fraction

$$p = \frac{P}{I}$$

Modified asymptotic estimator

$$p_{\mathrm{MAS}} = p - \varsigma^2 \frac{1 - e^{-p^2/\varsigma^2}}{2p}$$

Plaszczynski et al. (2014)

- Low polarization fractions in the Galactic Plane
- Some highly polarized regions, no material counterpart

Polarization angle

$$\psi = \frac{1}{2} \mathrm{atan}\left(-U, Q\right)$$

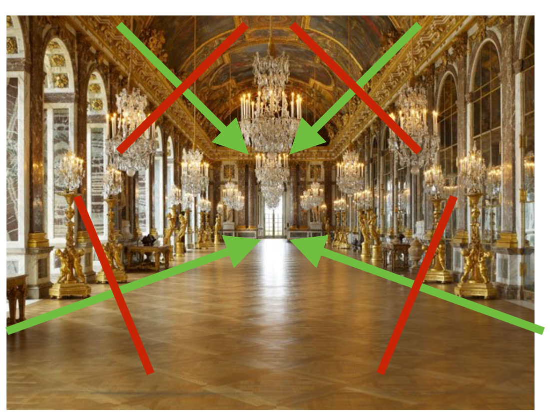

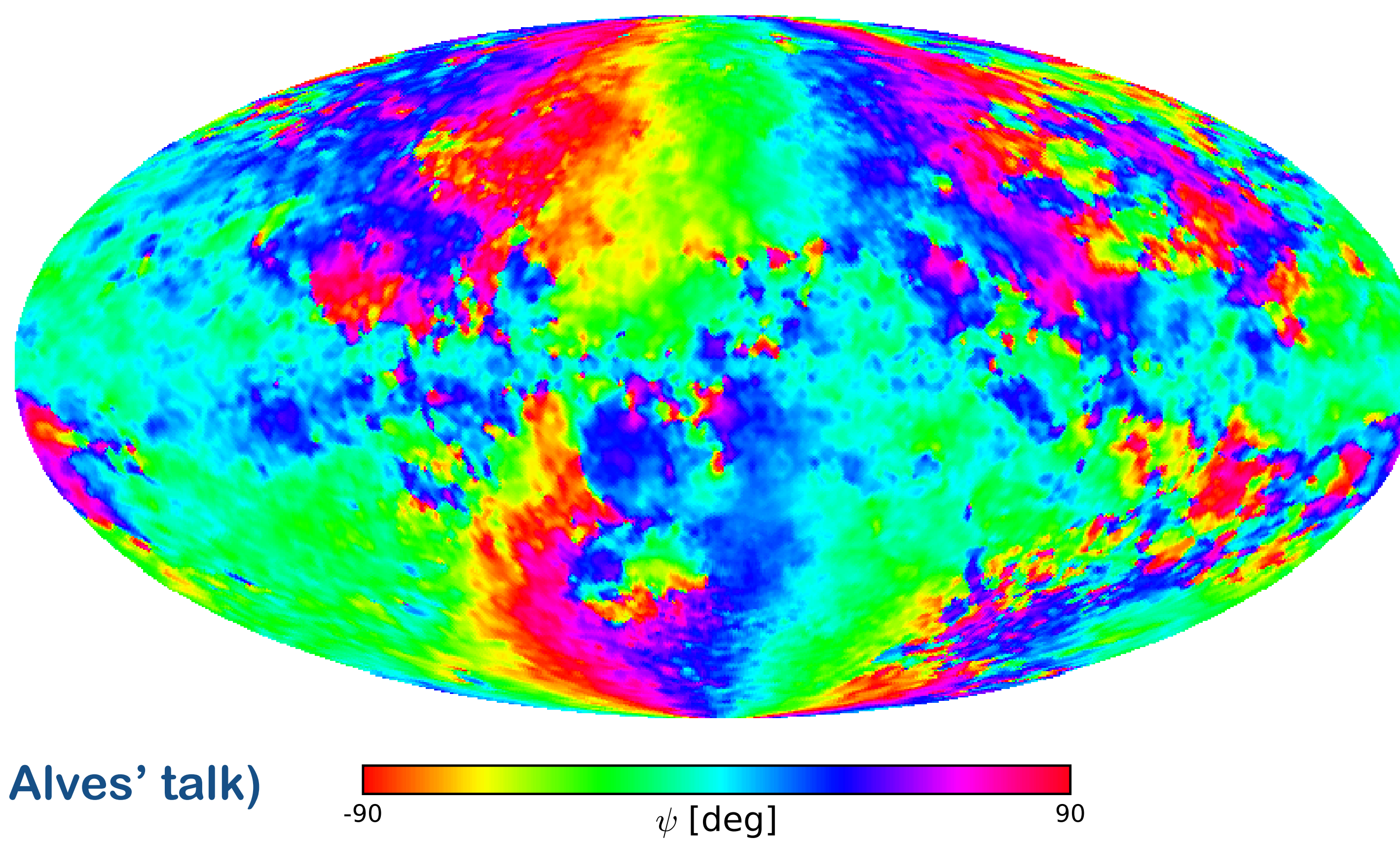

- B field along the Galactic plane
- Large-scale structure at high latitudes (see M. Alves' talk)

Spatial structure of the polarization angle map

Polarization angle dispersion function

$$\mathcal{S}(\boldsymbol{r},\delta) = \sqrt{\frac{1}{N}\sum_{i=1}^{N}\left[\psi(\boldsymbol{r}+\boldsymbol{\delta}_i)-\psi(\boldsymbol{r})\right]^2}$$

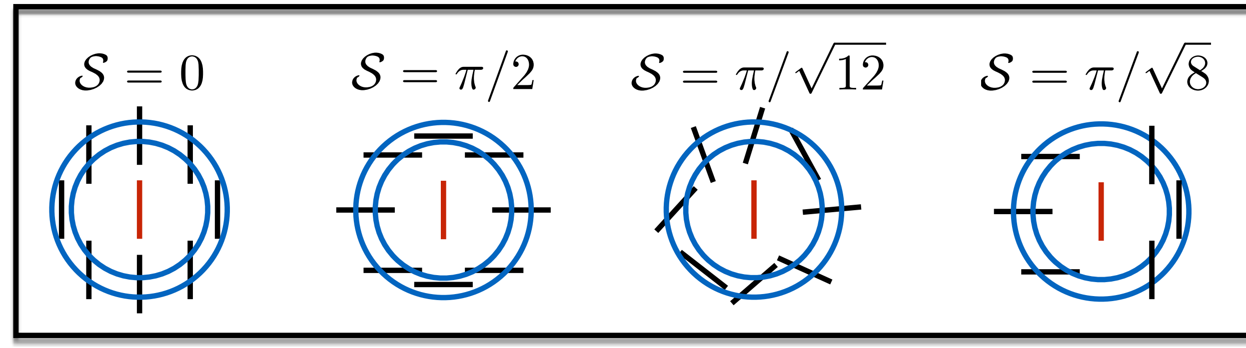

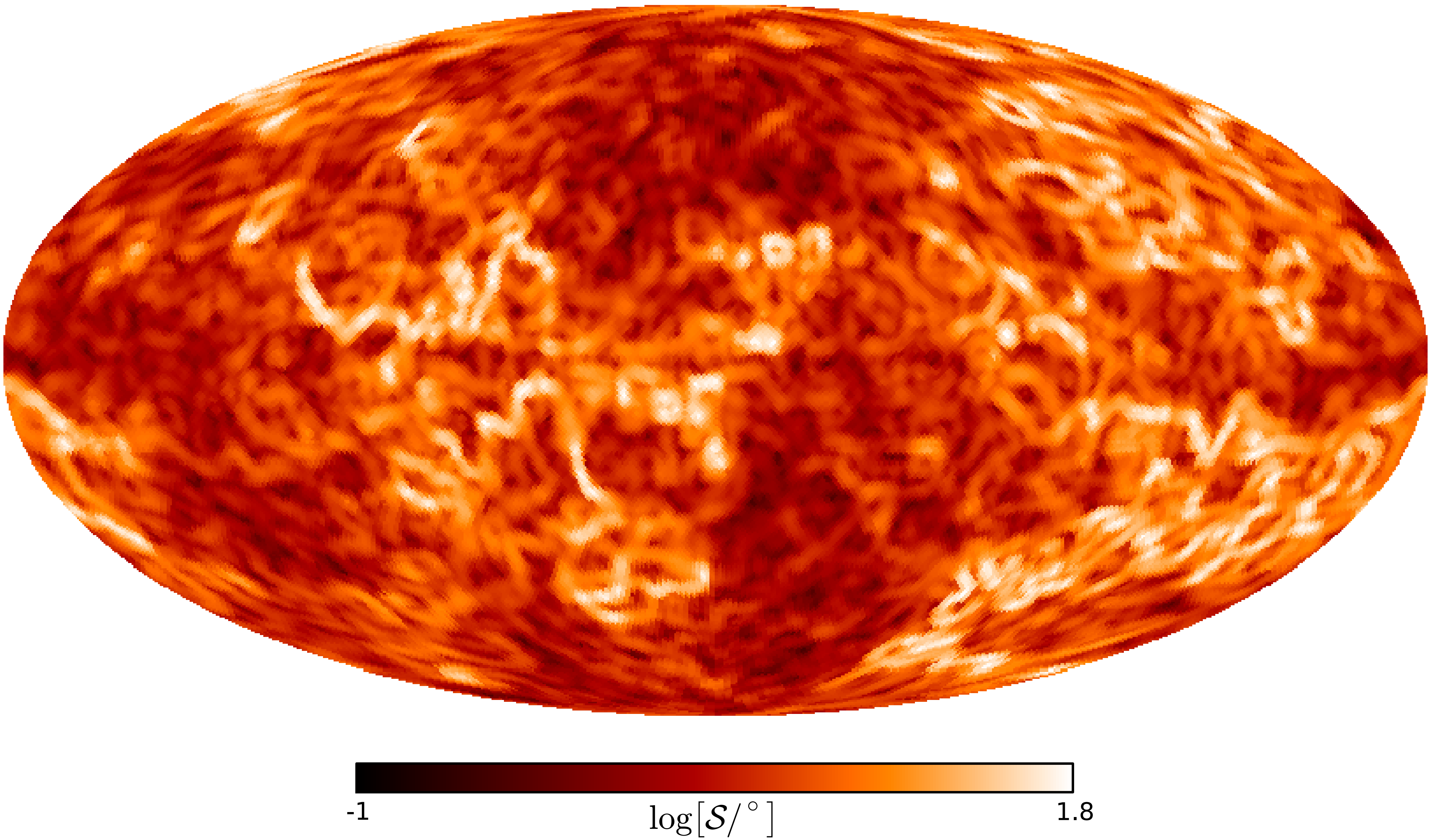

Planck Collaboration Int. XIX (2015)
Planck Collaboration XII (accepted)

- Strongly anti-correlated with the polarization fraction
- Low p where the polarization angle direction changes abruptly

One-point statistics of polarization fractions

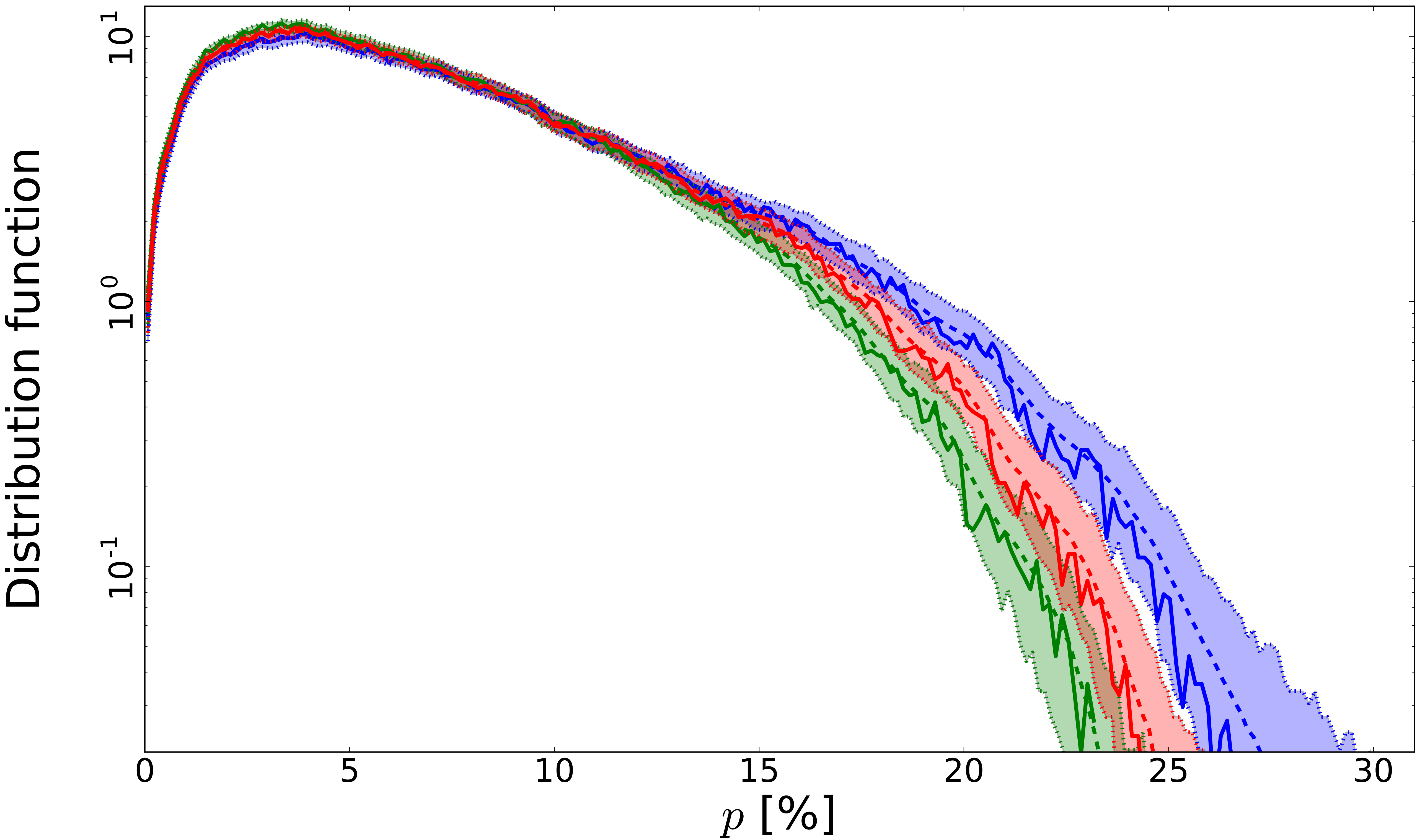

- Thick lines : data
- Coloured regions : span of DFs across a set of MC realizations
- Dotted lines : average DF across a set of MC realizations
- Different colours correspond to different total intensity offsets

Polarization fractions and column density

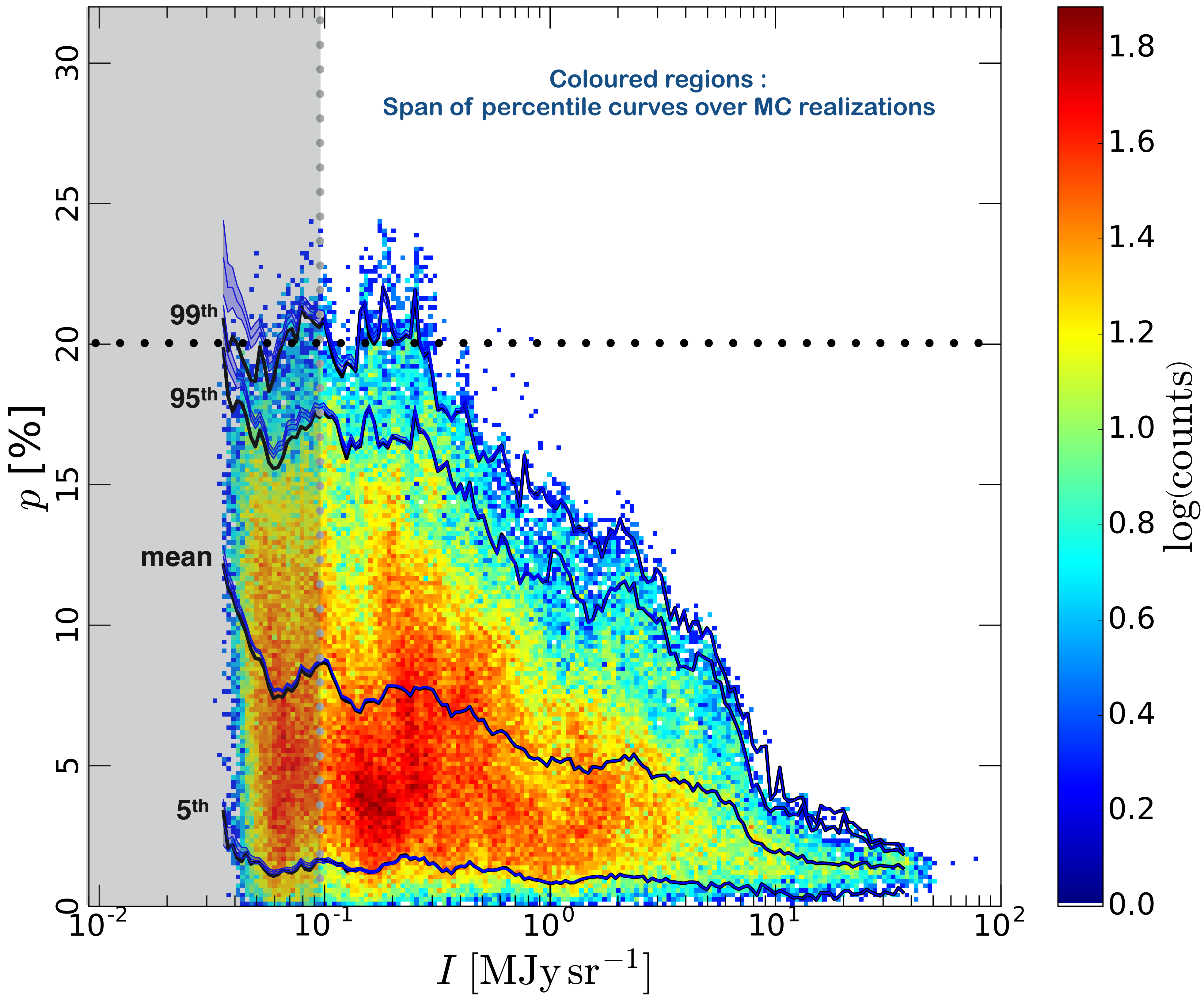

- Large scatter in the diffuse ISM
- Decrease of the polarization fraction towars more crowded or denser regions
- Low intensity end quite sensitive to offset : potential constraint ?

Polarization fractions and angle dispersions

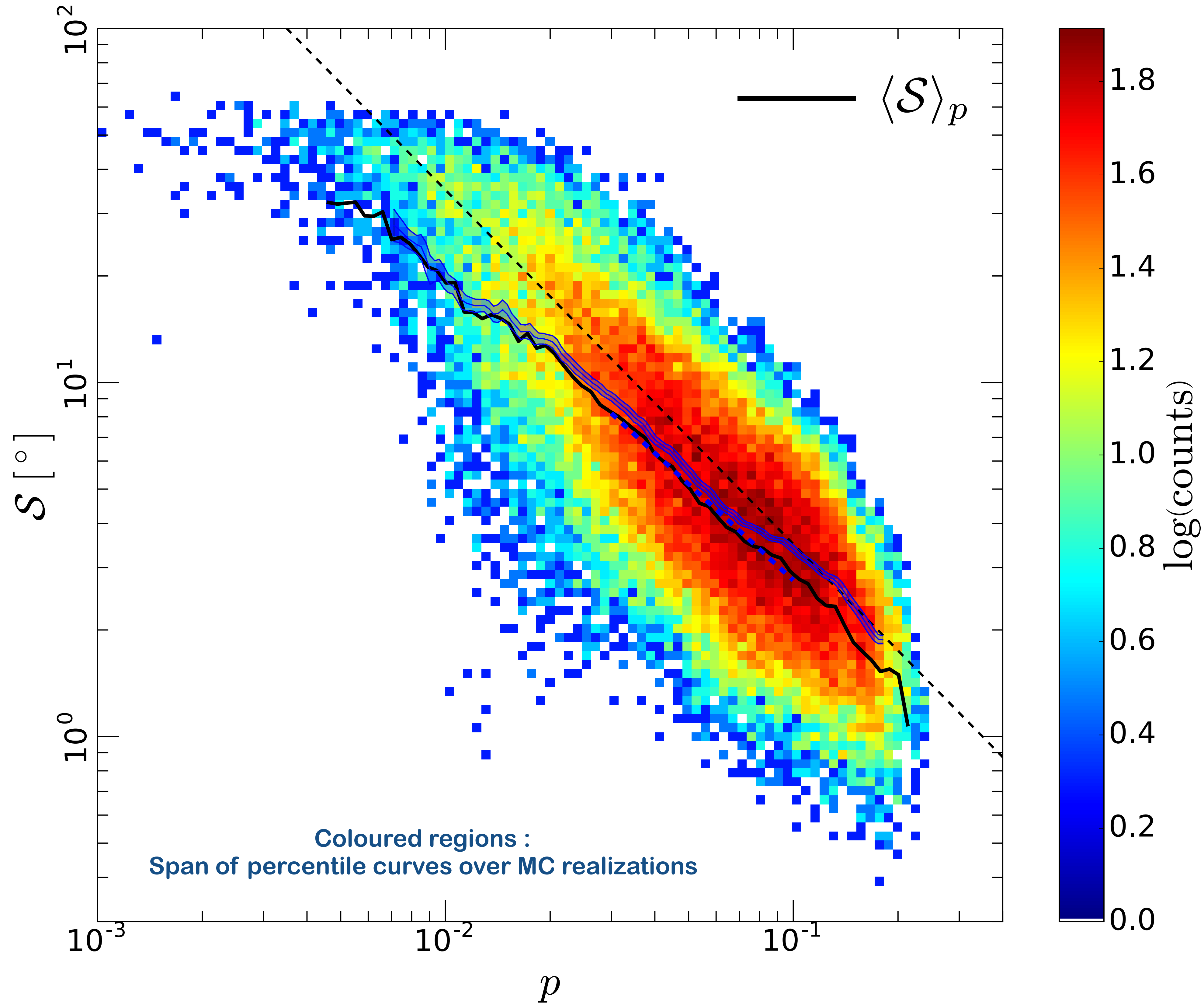

- Clear anti-correlation
- Consistent with findings of Planck Int. XIX (intermediate latitudes only)
- Reproduced by a simple phenomenological model

A phenomenological model of the Planck polarized sky

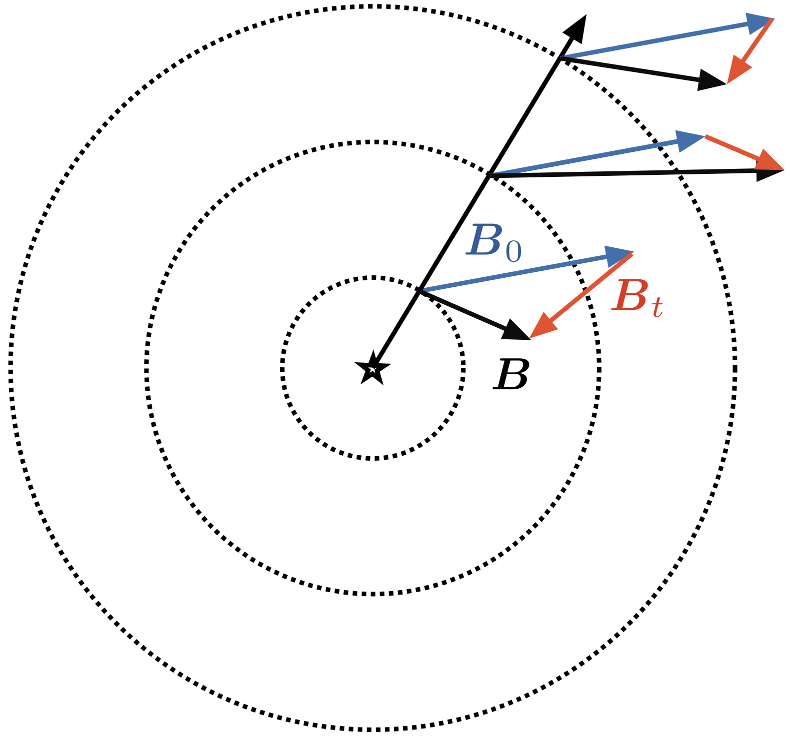

Magnetic field $B = B_0 + B_t$

Uniform field — Turbulent field

- A superposition of variously polarized layers (turbulent cells ?)
- Turbulent field : 3D Gaussian random variable
- Analysis of the Southern Galactic cap

  - Spatial power spectrum unconstrained $C_\ell \propto \ell^{\alpha_{\rm M}}$
  - Direction of the large-scale field $(l_0, b_0) = (70 \pm 5°, 24 \pm 5°)$
  - Turbulent-to-mean ratio $f_{\rm M} = 0.9 \pm 0.1$
  - Number of layers $N = 7 \pm 2$
  - Intrinsic polarization fraction $p_0 = 26 \pm 3\%$

U_{353}

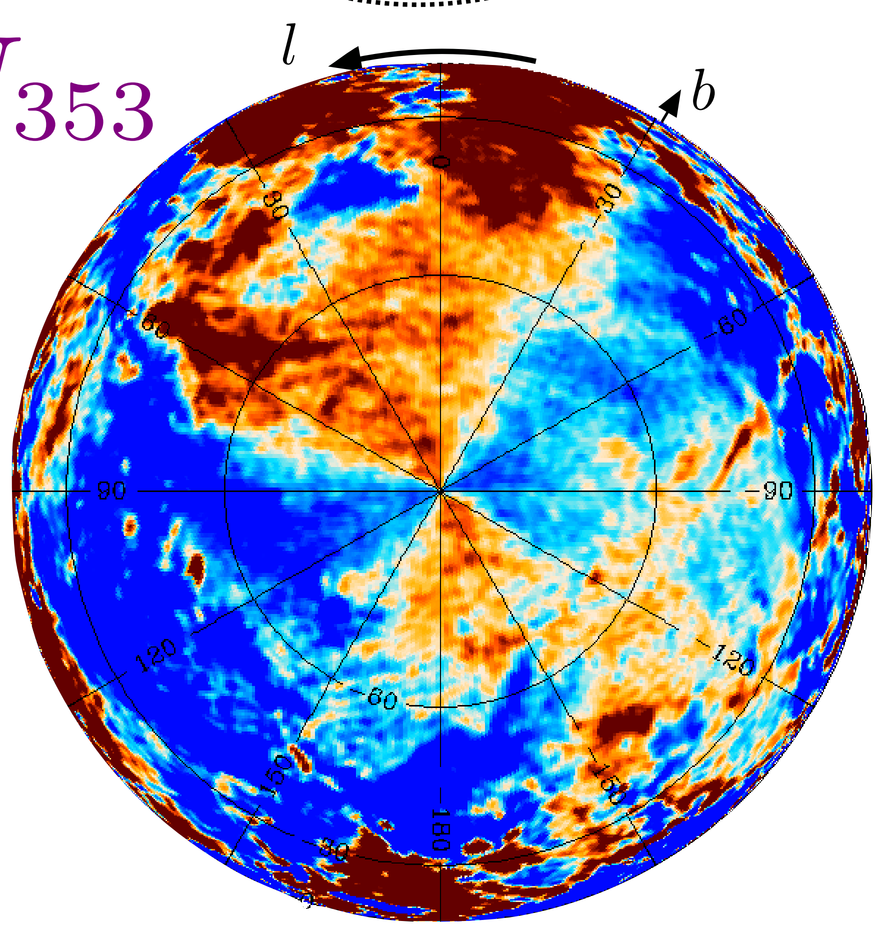

<u>Observations (black dots) vs. Simulations (colored regions)</u>

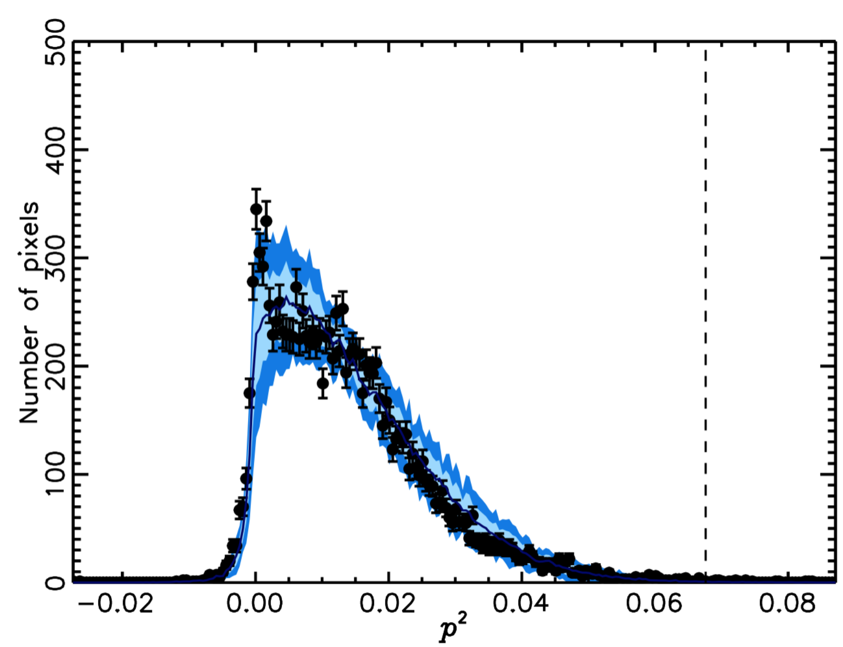

Polarization fraction

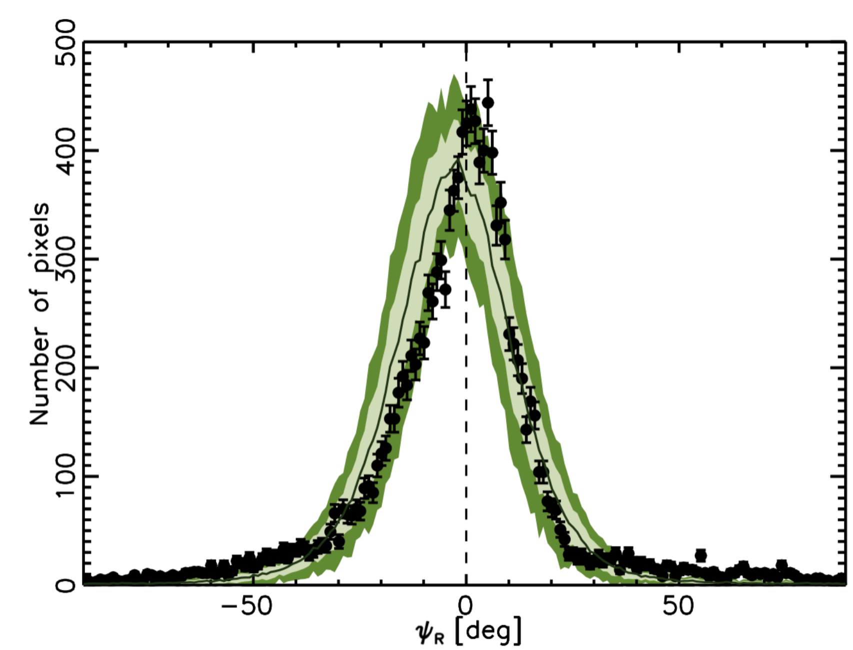

Polarization angle relative to the large-scale field

Planck Collaboration Int. XXXII, XLIV (2016)

Analytical derivation of the S vs p relation

S and p distribution in a model sky

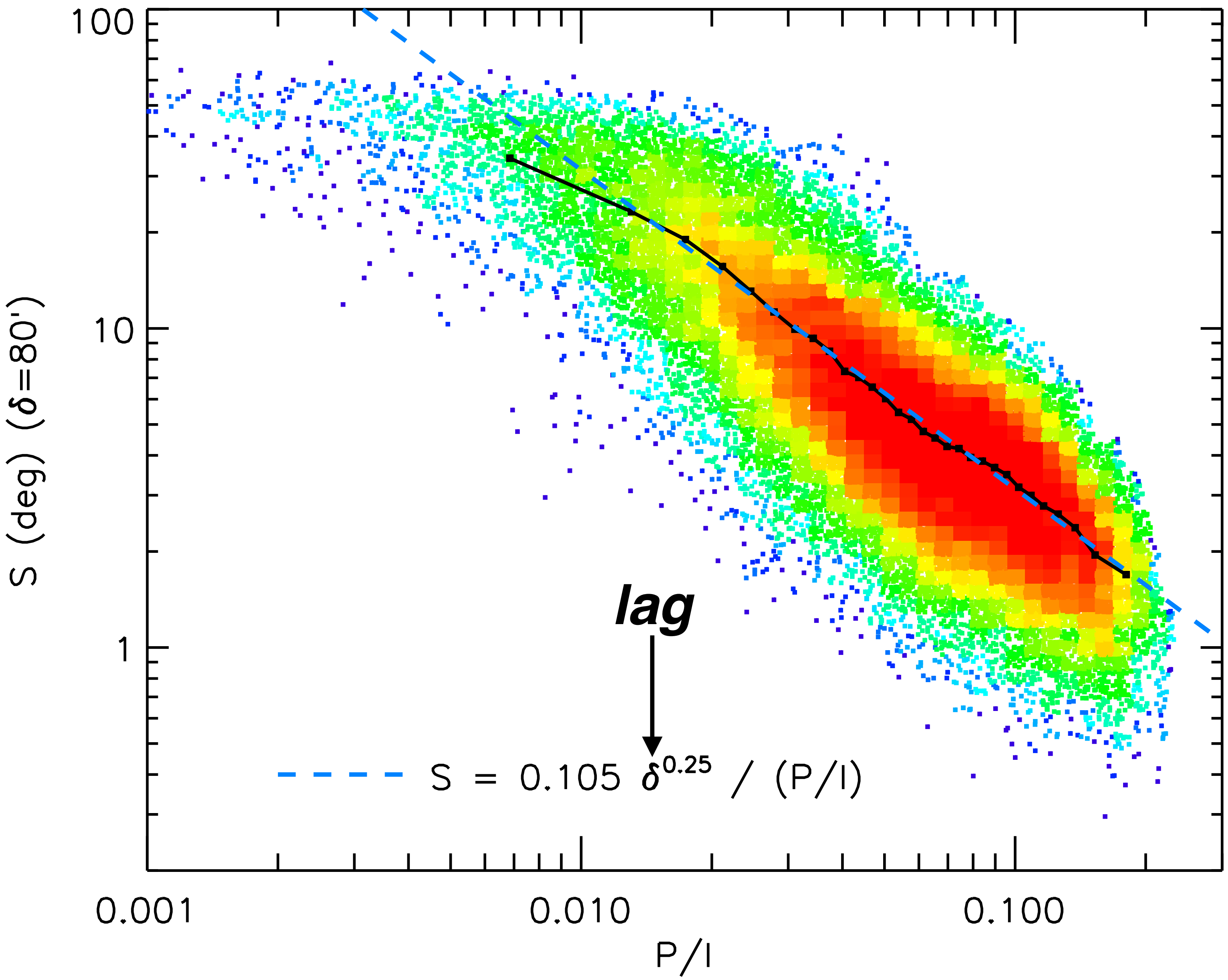

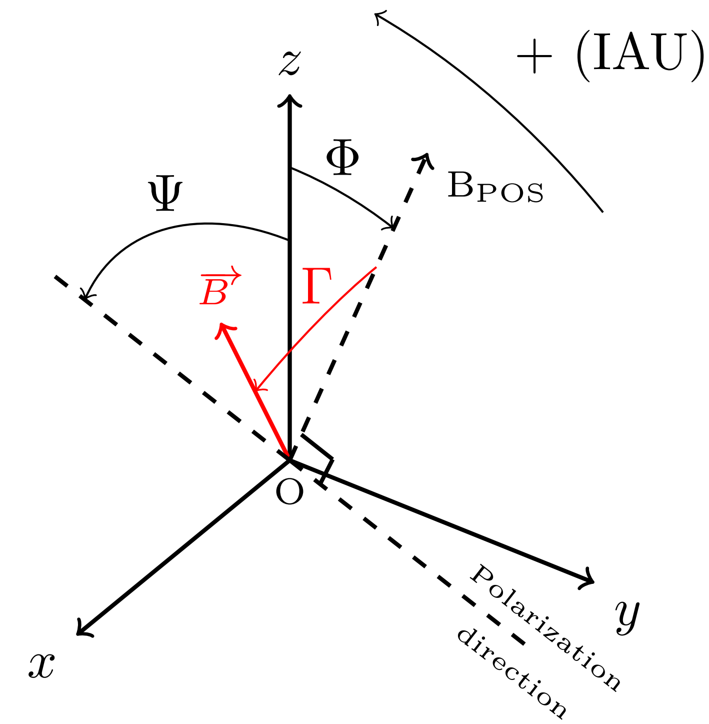

$$\langle \mathcal{S}(\ell) \rangle_p \simeq \frac{f_m(\ell)}{\sqrt{6N}} \frac{p_{\max}}{p}$$

where $f_m(\ell) = \dfrac{\delta B}{B_i}$

Because changes of dust properties or dust alignment are not included in either the Gaussian models or the synthetic observations from MHD simulations, we conclude that the anti-correlation between $\mathcal{S}$ and p must be a generic statistical property that results quite simply from the topology of the magnetic field alone.

Modelling polarized thermal dust emission with fBm fields

- Dust density and magnetic field modelled by 3D fields with realistic spatial correlations
- 9-parameter model (including spectral indices, fluctuation levels, angle of the mean field and depth on the LOS)
- Simulated polarization maps characterized by PDFs, power spectra, and correlations
- Monte-Carlo Markov Chain exploration of parameter likelihood given input polarization maps

Model parameters

Parameter	Prior [a]	Definition
β_B	$[1, 4]$	Spectral index of the 3D turbulent magnetic field
β_n	$[1, 5]$	Spectral index of the 3D dust density field
$\log_{10} y_n$	$[-1, 1]$	Log of the RMS-to-mean ratio of dust density
$\log_{10} y_B^{\mathrm{POS}}$	$[-1, 1]$	Log of the ratio of the turbulent magnetic field RMS to the mean magnetic field in the POS
χ_0	$[-90°, 90°]$	Position angle of the mean magnetic field in the POS
$\log_{10}(d/1\,\mathrm{pc})$	$[-0.3, 1.5]$ [b]	Depth of the simulated cube
$\log_{10}\left(\langle n_{\mathrm{H}}\rangle/1\,\mathrm{cm}^{-3}\right)$	$[1, 2.7]$ [c]	Mean dust density
T_{d}	$[5\,\mathrm{K}, 200\,\mathrm{K}]$	Dust temperature
p_0	$[0.01, 0.5]$	Intrinsic polarisation fraction parameter

Observables

Type	From
Mean values	τ_{353}, T_{obs}
Distribution function	I_{m}, Q_{m}, U_{m}, p_{MAS}, ψ, $\mathcal{S}$, $\tau_{353}/\langle\tau_{353}\rangle$
Power spectrum	I_{m}, Q_{m}, U_{m}
Correlation	$\{\mathcal{S}, p_{\mathrm{MAS}}\}$

Levrier et al. (2018)

MCMC fitting on the Polaris Flare Planck polarization maps

Parameters	β_B	β_n	$\log_{10} y_n$	$\log_{10} y_B^{\mathrm{POS}}$	χ_0 [°]	$\log_{10}\left(\frac{d}{1\,\mathrm{pc}}\right)$	$\log_{10}\left(\frac{\langle n_{\mathrm{H}}\rangle}{1\,\mathrm{cm}^{-3}}\right)$	T_{d} [K]	p_0	$\left\langle \chi^2_{\mathrm{best}} \right\rangle$
Best fit values	$2.8^{+0.2}_{-0.2}$	$1.7^{+0.4}_{-0.3}$	$0.2^{+0.2}_{-0.2}$	$-0.19^{+0.04}_{-0.04}$	-69^{+2}_{-3}	$1.1^{+0.3}_{-0.2}$	$1.6^{+0.2}_{-0.3}$	$17.5^{+0.5}_{-0.5}$	$0.12^{+0.02}_{-0.02}$	2.9

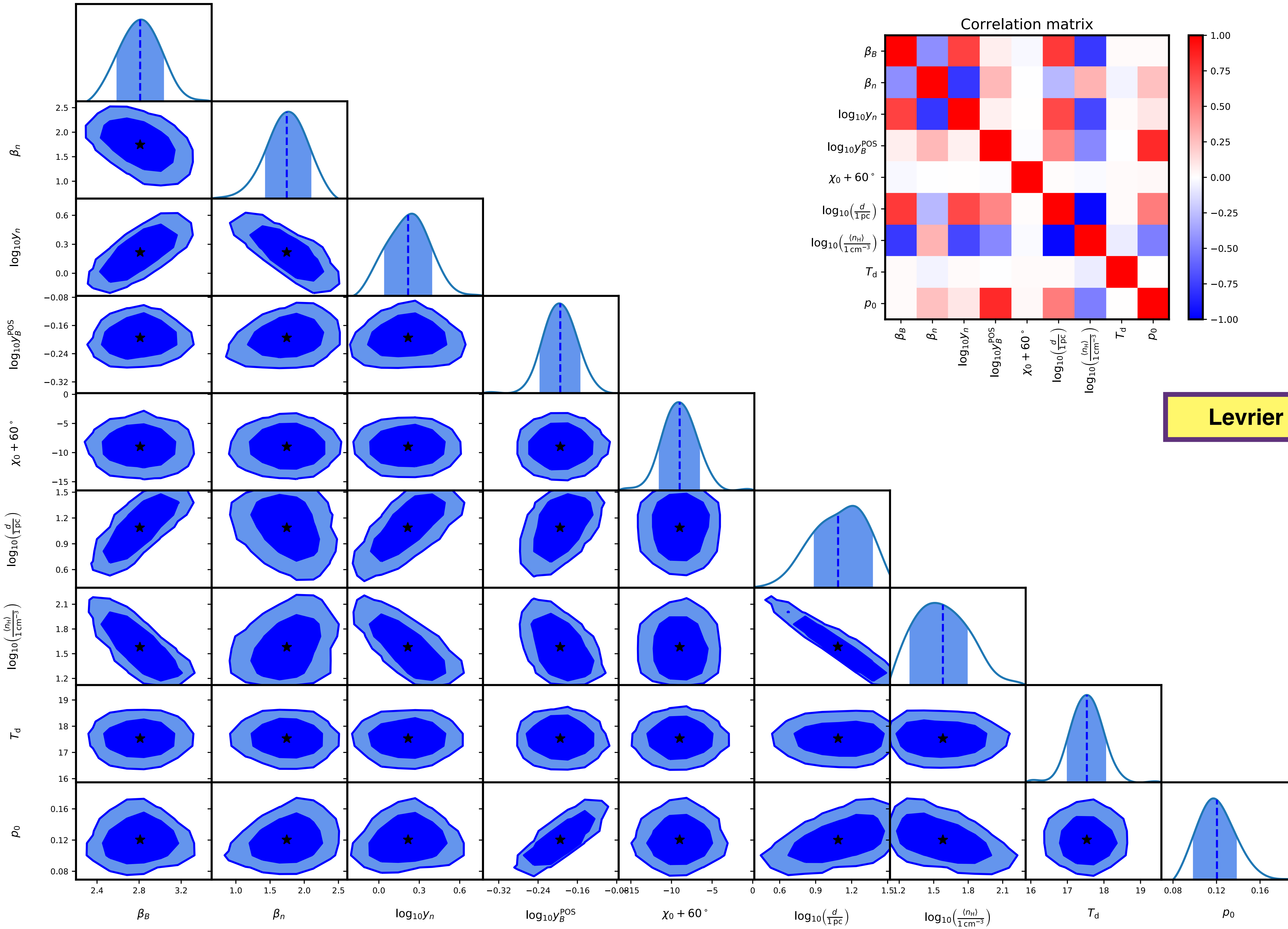

Levrier et al. (2018)

Orientation of magnetic field and structures of matter

- In nearby molecular clouds, using the Histogram of Relative Orientations (HRO) **Soler et al. (2013)**
- Change of relative orientation as column density increases
- Consistent with sub- and trans-Alfvénic simulations of MHD turbulence (strong magnetic field)
- Estimates of B from the Davis-Chandrasekhar-Fermi method **Chandrasekhar & Fermi (1953), Hildebrand et al. (2009)**

$$B_{\mathrm{POS}} \sim 10 - 50\,\mu\mathrm{G}$$

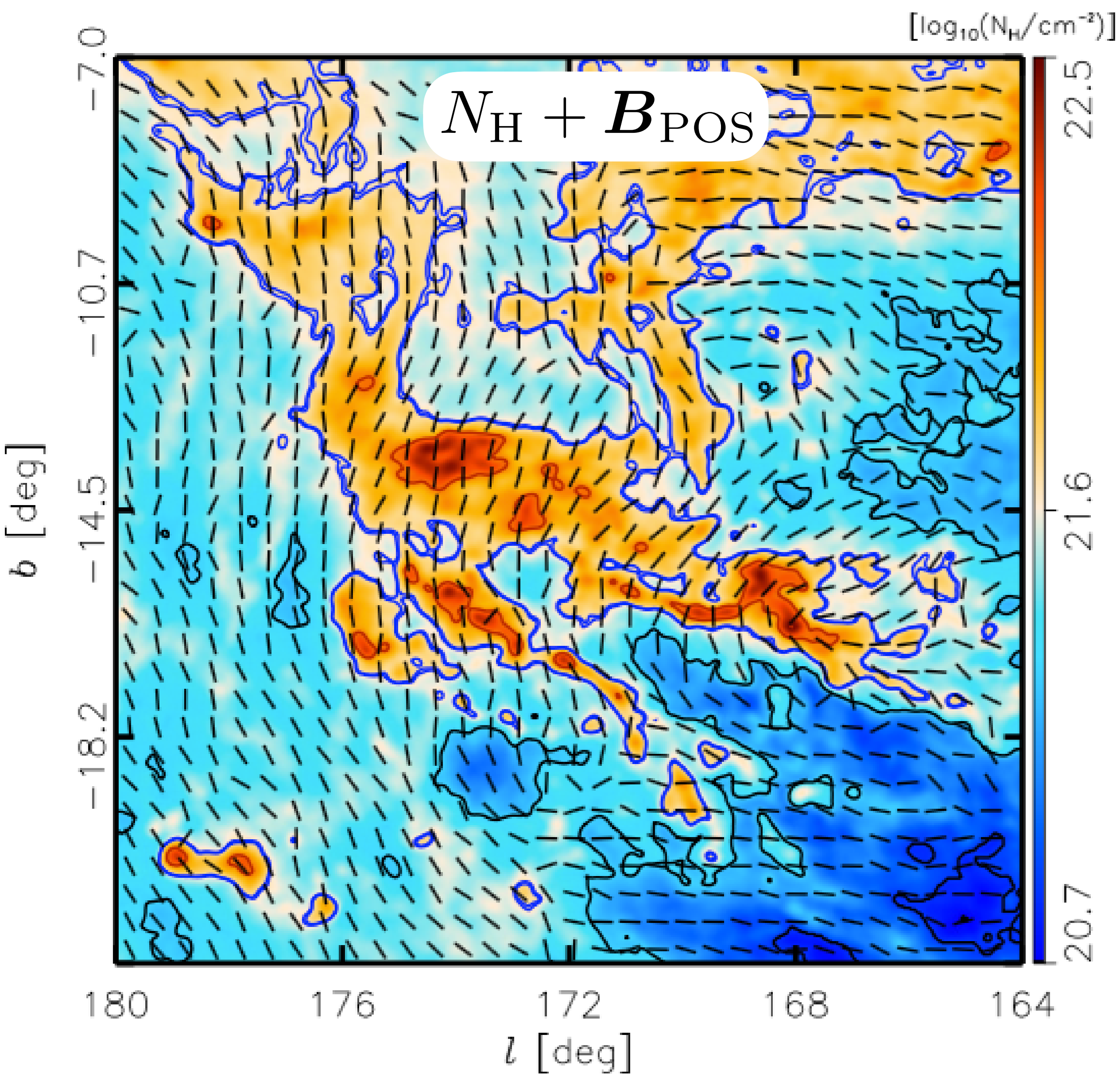

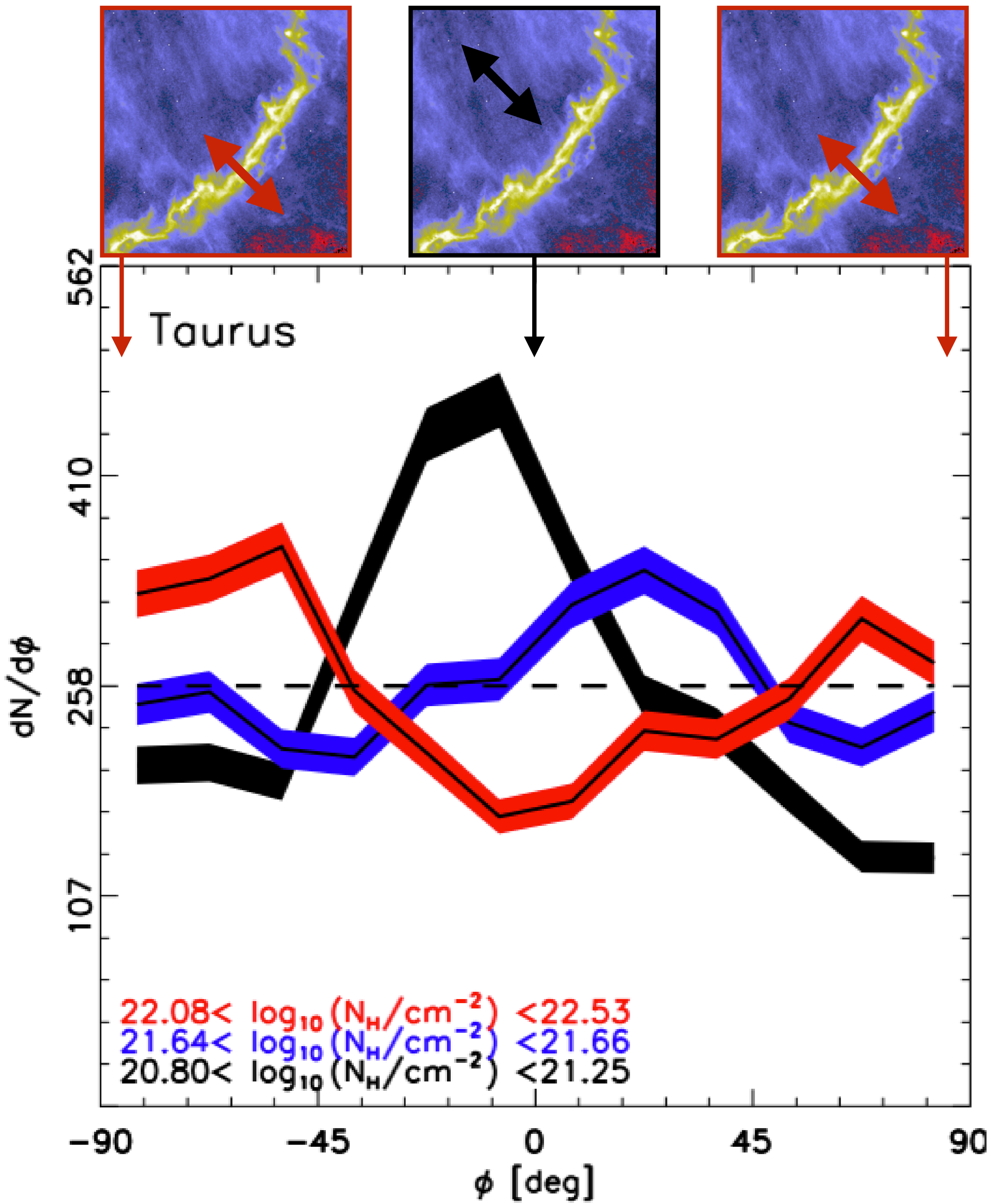

Planck Collaboration Int. XXXV (2016)

Orientation of magnetic field and structures of matter

- At intermediate and high Galactic latitudes, using the eigenvalues and eigenvectors of the Hessian
- Relative angle between filaments and magnetic field shows preferred alignment

$$\mathbf{H} = \begin{bmatrix} \partial^2_{xx} D_{353} & \partial^2_{xy} D_{353} \\ \partial^2_{xy} D_{353} & \partial^2_{yy} D_{353} \end{bmatrix}$$

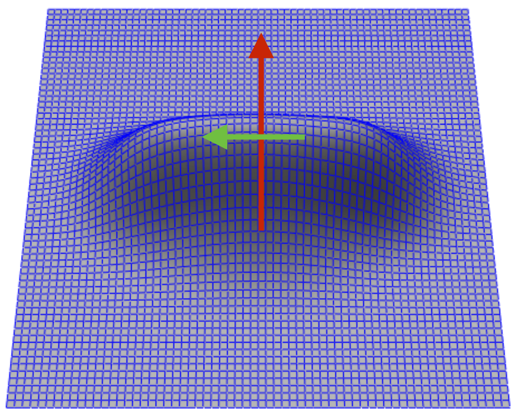

$$\langle p \rangle = 12 \pm 1\%$$

Map of the most negative eigenvalue

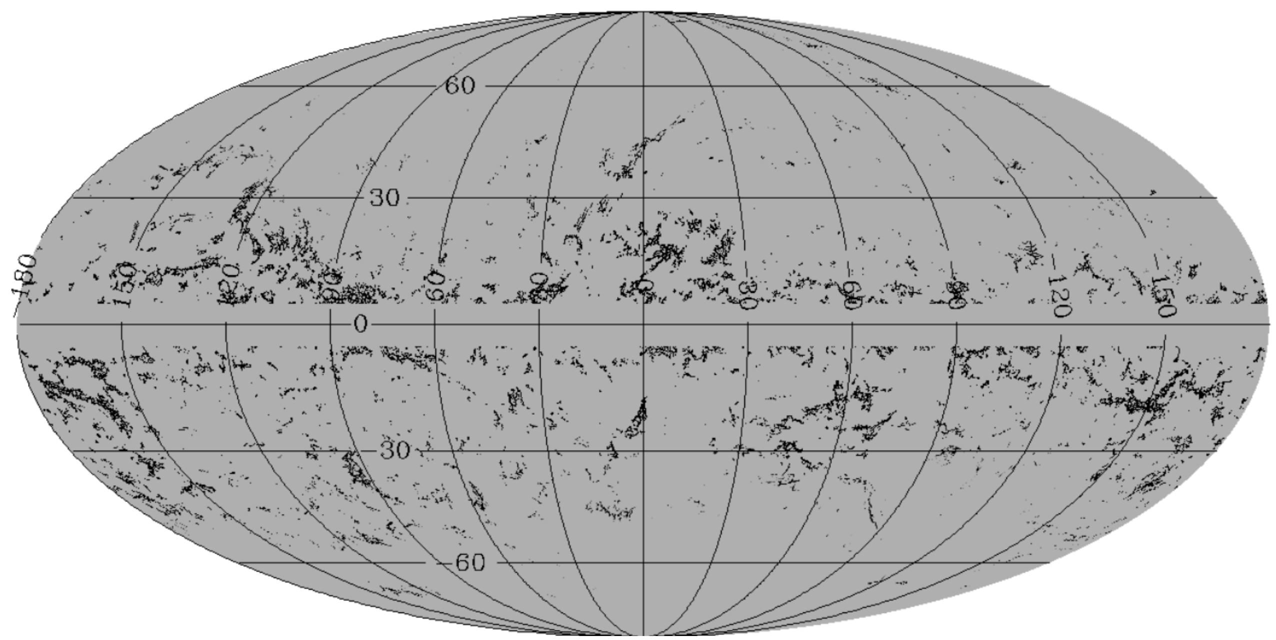

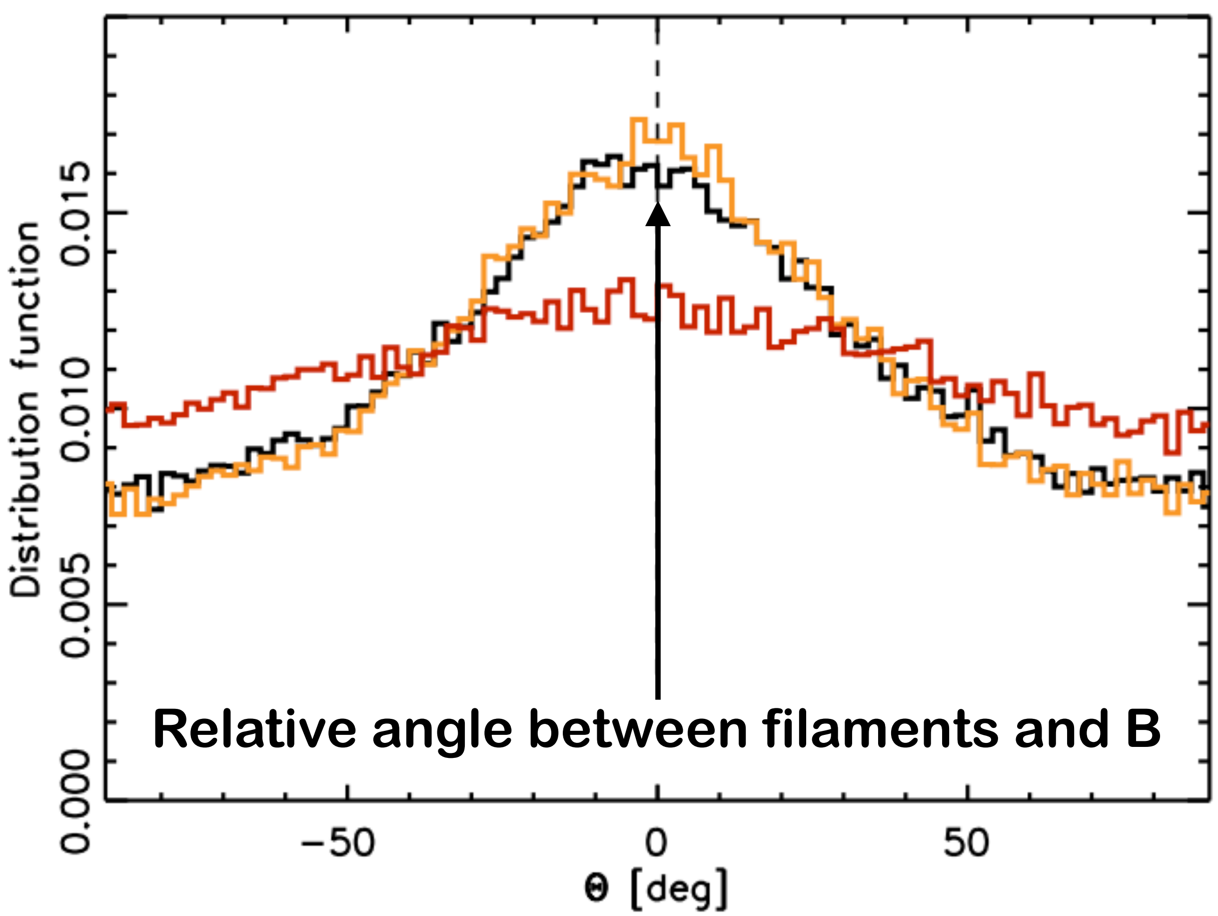

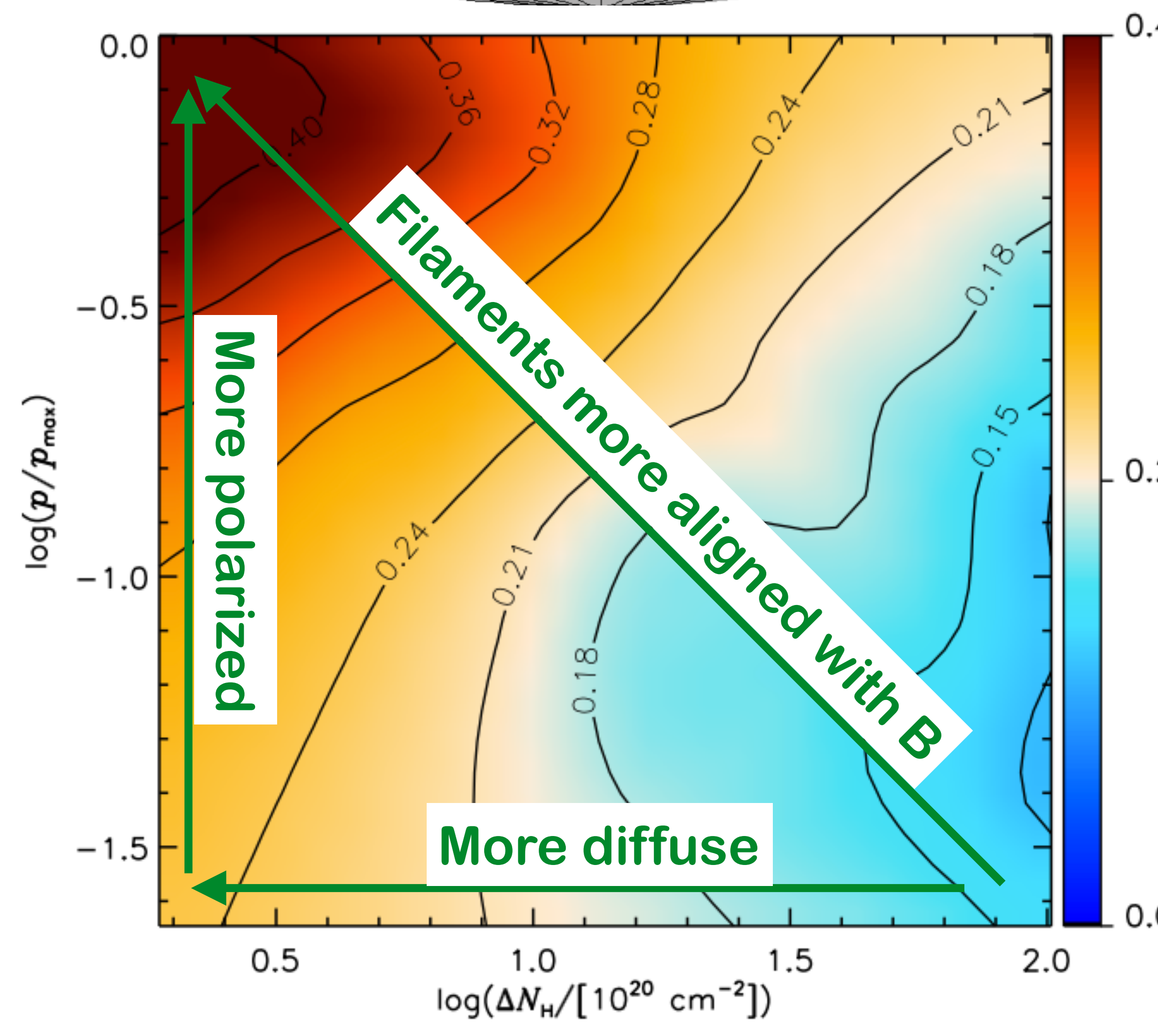

Planck Collaboration Int. XXXII (2016)